CHEMOSTAT PREDATOR-PREY MODEL WITH IVLEV FUNCTIONAL RESPONSE

A PREDATOR-PREY MODEL IN THE CHEMOSTAT WITH IVLEV FUNCTIONAL RESPONSE

By
TEDRA BOLGER, B. Sc.

A Thesis Submitted to the School of Graduate Studies in Partial Fulfilment
of the Requirements for the Degree Master of Science

McMaster University
September 2017

McMaster University, Hamilton, Ontario

MASTER OF SCIENCE (2017) (Mathematics)

TITLE: A Predator-Prey Model in the Chemostat with Ivlev Functional Response

AUTHOR: Tedra Bolger, B. Sc. (McGill)

SUPERVISOR: Professor G. S. K. Wolkowicz

NUMBER OF PAGES: vii, 66

Acknowlegements

I would first like to thank my supervisor, Dr. Wolkowicz for her patience and efforts in guiding my research.

Thank you to my parents, Spiro and Ann Daoussis, for their never ending love and encouragement. Also to my sister and best friend, Elise Bolger, for her support, and for making me smile every day.

Also a huge thank you to my friends Savannah Spilotro, Madeleine Hill, Brydon Eastman, and Aná Gradney. My time at McMaster would not have been nearly as much fun without the four of you.

Abstract

It has been shown that the classical Rosenzweig-MacArthur predator-prey model is sensitive to the functional form of the predator response. To see if this sensitivity remains in the highly controlled environment of the chemostat, we use a predator-prey model with three trophic levels and a Holling type II predator response function. We first focus on the analysis of the model using an Ivlev functional response. Local and global dynamics are studied, with global stability of the coexistence equilibrium point obtained under certain conditions. Bifurcation analysis reveals the existence of a stable periodic orbit that appears via a super-critical Hopf bifurcation. The uniqueness of this periodic orbit is explored. Finally, we make comparisons between the dynamics of the model with Ivlev response and Monod response, both of which have nearly identical graphs. The same sensitivity to functional form is observed in the chemostat as in the classical model.

List of Figures

Contents

Chapter 1

Background

Predator-prey models are a well studied tool used in population ecology. In particular, the experimental evidence and predictions of mathematical models can be seen in [3, 4, 6]. Predator-prey theory can be traced back to the Lotka-Volterra equation [21, 31]. The Rosenzweig-MacArthur model was then developed by expanding to include density dependent prey growth and Holling type functional responses [27], and its effectiveness in producing realistic dynamic behaviour has been shown [30]. This model predicts that increasing the availability of nutrients can cause the dynamics to shift from a stable equilibrium to oscillatory dynamics [26]. A generalized version of this Rosenzweig-MacArthur model is also commonly studied [28, 8]. Collectively, the Rosenzweig-MacArthur and the generalized Rosenzweig-MacArthur models can be referred to as the classical predator-prey model.

An issue with modelling arises since the explicit mathematical expressions required to make biological models rigorous are not always known. This is true in particular for the function which describes the uptake of resources. Moreover, it has been determined that, depending on which functional form is chosen, the model can predict qualitatively and quantitatively different dynamics. This problem is observed and detailed in [9] by Fussmann and Blasius. They study the classical predator-prey model with three functional responses, namely the Monod [25], Ivlev [15], and Trigonometric [16] functional responses. These functions are chosen as they are nearly indistinguishable for appropriate parameter choices, and they all have Holling type II form. Fussmann and Blasius showed that qualitative and quantitative dynamics predicted by the model can be different depending on which of the functional forms was used. Their result was explained further in [28] by Seo and Wolkowicz who used a

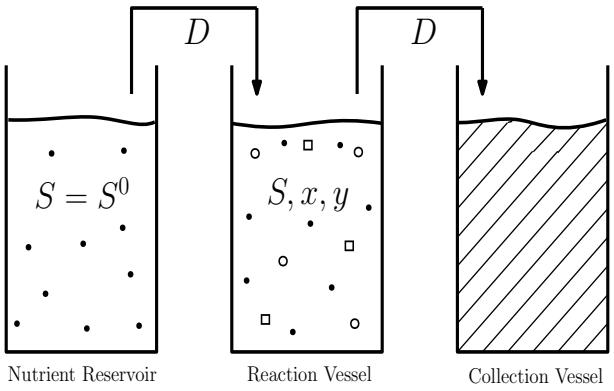

Figure 1.1: *A simple diagram of a chemostat. The nutrient reservoir has substrate concentration S^0, which is then pumped into the reaction vessel at rate D. The reaction vessel contains prey and predator populations. Contents of the reaction vessel are pumped out at the same rate D to maintain constant volume.*

rigorous bifurcation approach to study the extreme sensitivity of the classical predator-prey model to the functional form for resource uptake.

The motivation for this thesis comes from the work of Fussmann and Blasius in the sense that we wish to see if this sensitivity to functional form remains, even in the highly controlled environment of the chemostat. A detailed description of the chemostat is given in [29]. Simply put, the chemostat is a laboratory apparatus used for the continuous culture of organisms. It consists of three vessels; a nutrient reservoir, reaction vessel, and collection vessel. In all our models we assume that the reaction vessel is perfectly mixed, thus there is no spatial variation in the concentrations of the populations. It is assumed that the growth of the prey population is limited by a single nutrient, that is pumped into the reaction vessel at a rate D. So as to maintain constant volume in the reaction vessel, the contents are removed to the collection vessel at the same rate D. Figure 1.1 gives a simplified depiction of the chemostat. It is also assumed that the death rate of the species is insignificant compared to the dilution rate, and that all external factors are held constant.

Here we consider a model of the chemostat with three distinct trophic levels. That is, the reaction vessel contains both a prey species that feeds only on the nutrient, and a predator species that feeds only on the prey. While the motivation comes from studying different resource uptake functional forms, this thesis focuses specifically on proving the dynamics for the Ivlev functional response. Comparisons with the dynamics from the Monod functional form

are also made. The differences between the dynamics predicted using these functional forms are of particular significance since the prey isocline in both cases has at most a single extremum.

This thesis is organized in the following way. In Chapter 2 we give a mathematical description of the model and its necessary assumptions. In addition we give a non-dimensional version of the model and examine its limiting systems. Chapter 3 focuses on a full analysis of the possible configurations of the prey nullcline. The local and global stability of equilibria is studied in Chapter 4. These results draw on Lyapunov functions, the LaSalle Extension Theorem, and the Dulac Criterion. Chapter 5 is dedicated to existence and uniqueness of the periodic orbit. The Poincaré criterion and Liénard function theory are used. In particular, an adapted version of Zhang's theorem by Kooij and Zegeling [17] is used. For the Ivlev response the proof for uniqueness of the periodic orbit is not complete, but certain conditions for the uniqueness are established. Bifurcation analysis is done in Chapter 6. The existence and criticality of the Hopf bifurcation is determined, as well as the sequence of bifurcations that can occur. Next, Chapter 7 focuses on extending the stability results from the two dimensional limiting system model, back to the original three dimensional model using the Butler-McGehee Lemma. Finally, Chapter 8 begins by establishing some preliminary analysis for the Monod functional response. A proof for uniqueness of the periodic orbit when the coexistence equilibrium is unstable is given. As a corollary to this theorem, we get that whenever the coexistence equilibrium point is locally stable, it is globally stable. The chapter concludes with a comparison between the dynamics from the Ivlev response and the Monod response.

Chapter 2

Introduction

2.1 The Model

The predator-prey model we consider is:

$$\begin{aligned} S'(t) &= (S^0 - S)D - xp(S) \\ x'(t) &= x(-D + \gamma p(S)) - yq(x) \\ y'(t) &= y(-D + \delta q(x)) \\ S(0) &> 0, \quad x(0) > 0, \quad y(0) > 0. \end{aligned} \tag{2.1}$$

The model is based on a chemostat with three trophic levels. The dependent variables $S(t)$, $x(t)$ and $y(t)$ represent the concentration of substrate, prey and predator respectively, in the growth chamber at time t. It is assumed that the trophic levels are distinct so that the prey feeds only on the substrate and the predator feeds only on the prey. It is also assumed that the growth vessel is perfectly stirred so there are no spatial variations in the concentrations of substrate or either population. The concentration of substrate in the nutrient reservoir is given by S^0, and D represents the rate of both inflow and outflow from the growth chamber. The parameters γ and δ represent yield constants for the consumption of substrate and the consumption of prey, respectively. In order to maintain biological relevance, it is assumed that all initial concentrations are positive. The function $p(S)$ represents substrate-uptake by the prey. The rate of conversion of the substrate into prey biomass is given by $\gamma p(S)$.

The function $p(S)$ satisfies the following:

$$\begin{aligned} &p(S) \text{ is continuously differentiable,} \\ &p(0) = 0, \\ &p(S) > 0 \text{ for } S > 0 \\ &p'(S) > 0 \text{ for } S \geq 0. \end{aligned} \tag{2.2}$$

We make the simplifying assumption that $p(S) = mS$, for constant $m > 0$. This choice for $p(S)$ is one of the simplest forms which satisfies the above assumptions. In a similar fashion the predator response function is denoted $q(x)$, and has the following properties:

$$\begin{aligned} &q(x) \text{ is continuously differentiable,} \\ &q(0) = 0, \\ &q'(x) > 0 \text{ for } x \geq 0, \\ &q''(x) < 0 \text{ for } x \geq 0. \end{aligned} \tag{2.3}$$

To study the sensitivity of this model to the functional form selected for $q(x)$, two different response functions are observed. This thesis focuses primarily on the Ivlev functional response that has the form $q_I(x) = a_I(1 - e^{-b_I x})$ [15]. Comparisons are then drawn between this Ivlev form and the Monod functional response that is given by $q_M(x) = \frac{a_M x}{b_M + x}$ [25]. Both Monod and Ivlev predator responses satisfy the required properties for a Holling Type II function given in (2.3), and are nearly indistinguishable when using nonlinear least squares optimization to fit the parameters to sample data of this type.

2.2 The Scaled Model

The system (2.1) with Ivlev functional response can be simplified by a change of variables. There are four variables (S, x, y and t) in the system so four parameters can be chosen to scale. Let $\hat{S} = \sigma S$, $\hat{x} = \alpha x$, $\hat{y} = \beta y$ and $\hat{t} = \tau t$. Then,

$$\begin{aligned} \frac{d\hat{S}}{d\hat{t}} &= \frac{\sigma}{\tau}((S^0 - S)D - mxS) = (\sigma S^0 - \hat{S})\frac{D}{\tau} - \frac{m}{\alpha\tau}\hat{x}\hat{S} \\ \frac{d\hat{x}}{d\hat{t}} &= \frac{\alpha}{\tau}(x(-D + \gamma m S) - ya(1 - e^{-bx})) = \hat{x}\left(-\frac{D}{\tau} + \frac{\gamma m}{\sigma\tau}\hat{S}\right) - \frac{a\alpha}{\beta\tau}\hat{y}\left(1 - e^{-\frac{b}{\alpha}\hat{x}}\right) \\ \frac{d\hat{y}}{d\hat{t}} &= \frac{\beta}{\tau}(y(-D + \delta a(1 - e^{-bx})) = \hat{y}\left(-\frac{D}{\tau} + \frac{\delta a}{\tau}(1 - e^{-\frac{b}{\alpha}\hat{x}})\right). \end{aligned}$$

Taking $\hat{D} = \frac{D}{\tau}$, $\hat{S^0} = \sigma S^0$, and $\hat{b} = \frac{b}{\alpha}$ gives

$$\begin{aligned}
\frac{d\hat{S}}{d\hat{t}} &= (\hat{S^0} - \hat{S})\hat{D} - \frac{m}{\alpha\tau}\hat{x}\hat{S} \\
\frac{d\hat{x}}{d\hat{t}} &= \hat{x}(-\hat{D} + \frac{\gamma m}{\sigma\tau}\hat{S}) - \frac{a\alpha}{\beta\tau}\hat{y}(1 - e^{-\hat{b}\hat{x}}) \\
\frac{d\hat{y}}{d\hat{t}} &= \hat{y}(-\hat{D} + \frac{\delta a}{\tau}(1 - e^{-\hat{b}\hat{x}})).
\end{aligned}$$

To eliminate a, b, γ and δ choose $\sigma = \gamma b$, $\alpha = b$, $\beta = \frac{b}{\delta}$ and $\tau = \delta a$, and take $\hat{m} = \frac{am\gamma}{b}$. Then the system (with hats omitted to simplify notation) is reduced to

$$\begin{aligned}
\frac{dS}{dt} &= (S^0 - S)D - mxS \\
\frac{dx}{dt} &= x(-D + mS) - y(1 - e^{-x}) \\
\frac{dy}{dt} &= y(-D + 1 - e^{-x}).
\end{aligned} \tag{2.4}$$

The choice to scale out γ and δ is for convenience. Choosing to eliminate a and b is arbitrary. At some points to simplify analysis it may be more useful to choose a different scaling of the variables. An alternate scaling is used in Chapter 8.

2.3 Well-Posedness

As system (2.1) represents a biological system we require all solutions to be non-negative and bounded for all time when given relevant initial conditions.

Lemma 2.1. *The solutions $S(t)$, $x(t)$ and $y(t)$ of system (2.4) are bounded and non-negative.*

Proof. The vector field given by System (2.4) is continuously differentiable in the first octant $\{(S, x, y) : S, x, y \geq 0\}$, implying that solutions with non-negative initial conditions exist and are unique. To establish non-negativity of the substrate concentration assume $S(\tau) = 0$ for some $\tau \geq 0$. Then $S'(\tau) = S^0 D > 0$ so the solution $S(t)$ remains in the positive octant $\forall t \geq 0$. For the predator and prey populations, note that the $(S, 0, y)$ and the $(S, x, 0)$ planes are invariant. By uniqueness of solutions these planes cannot be reached in

finite time for trajectories originating in the interior of $\mathbb{R}^3$. As such $x(t) \geq 0$ and $y(t) \geq 0 \; \forall \; t \geq 0$. To prove boundedness of the solution consider the sum of solutions. Let $z(t) = S'(t) + x'(t) + y'(t)$. Adding the equations in (2.4) we obtain

$$z'(t) = D(S^0 - z(t)).$$

This is a first order differential equation with solution for $z(t)$ given by

$$z(t) = (z(0) - S^0)e^{-Dt} + S^0, \tag{2.5}$$

where $z(0) = S(0)+x(0)+y(0)$. Therefore $z \leq \max\{z(0), S^0\}$. Since the initial conditions for S, x and y are positive and the sum of the solutions is bounded above, the solutions $S(t)$, $x(t)$ and $y(t)$ are bounded in the biologically relevant octant. □

2.4 The Limiting Systems

The system in (2.4) can be further simplified by studying the limiting system. Note that from (2.5) the sum of solutions $S(t) + x(t) + y(t)$ converges to S^0 as $t \to \infty$. The ω-limit set is given by

$$\omega = \{(S, x, y) \; \in \; \overline{\mathbb{R}^3_+} : \; \exists \text{ an increasing, unbounded sequence } t_k \text{ such that } (S(t_k), x(t_k), y(t_k)) \to (S, x, y) \text{ as } k \to \infty\}.$$

It follows from (2.5) that $S(t_k) + x(t_k) + y(t_k) \to S + x + y = S^0$. Therefore ω is restricted to the $\{(S, x, y) : S + x + y = S^0\}$ simplex. We will first study the dynamics of system (2.4) restricted to the two dimensional simplex. Chapter 7 focuses on expanding this analysis to the full three dimensional system. Three identical limiting systems can be obtained by eliminating one of the variables using the relationship $S + x + y = S^0$. First eliminate y to obtain the S, x subsystem.

$$\begin{aligned} \frac{dS}{dt} &= (S^0 - S)D - mxS \\ \frac{dx}{dt} &= x(-D + mS) - (S^0 - S - x)q(x) \end{aligned} \tag{2.6}$$

$$S(0) \geq 0, \quad x(0) \geq 0.$$

Similarly, obtain the S, y subsystem by eliminating x:

$$\begin{aligned} \frac{dS}{dt} &= (S^0 - S)D - (S^0 - S - y)mS \\ \frac{dy}{dt} &= y(-D + q(S^0 - S - y)) \end{aligned} \tag{2.7}$$

$$S(0) \geq 0, \quad y(0) \geq 0.$$

Finally obtain the x, y subsystem by eliminating S:

$$\begin{aligned} \frac{dx}{dt} &= x(-D + m(S^0 - x - y)) - yq(x) \\ \frac{dy}{dt} &= y(-D + q(x)) \end{aligned} \tag{2.8}$$

$$x(0) \geq 0, \quad y(0) \geq 0.$$

The most useful subsystem to study is the x, y subsystem in (2.8) since the predator nullcline is vertical. This planar system has properties similar to the classical Rosenzweig MacArthur predator-prey model [27] given by

$$\begin{aligned} \frac{dx}{dt} &= rx\left(1 - \frac{x}{K}\right) - yq(x) \\ \frac{dy}{dt} &= y(-D + q(x)) \end{aligned} \tag{2.9}$$

$$x(0) \geq 0, \quad y(0) \geq 0.$$

In this model, D is the death rate of the predator, r is the intrinsic growth rate of the prey, and K is the carrying capacity of the prey in the absence of the predator population. Also, x and y are the densities of the prey and predator populations, respectively, and $q(x)$ is the capture rate of the predator. It is assumed that the conversion rate of captured prey is proportional to the capture rate. The proportionality constant has been scaled out in the model presented here. The only difference between systems (2.8) and (2.9) is the term describing how the prey grows in the absence of the predator.

The remainder of this thesis focuses on the analysis of subsystem (2.8). By the conservation law from (2.5), there is a $1:1$ correspondence between the equilibria of the two dimensional subsystem (2.8) and the original three dimensional model (2.4). The local stability results are also equivalent. Boundedness

and non-negativity of solutions of (2.8) follow immediately from these results for (2.4) from (2.1). Further justification of the equivalence of the dynamics of these systems is given in Chapter 7.

The predator nullcline is given by the vertical line $x = q^{-1}(D)$. With the Ivlev response, this is $x = -\ln(1 - D)$. In order to have biologically relevant and interesting solutions we impose the restriction that the predator nullcline lies in the interior of the positive quadrant. For the Ivlev functional response this corresponds to restricting $0 < D < 1$.

To obtain an expression for the prey nullclines, the x' equation in (2.8) can be factored as:

$$x' = (mx + q(x))(F(x) - y), \tag{2.10}$$

where $y = F(x) \triangleq \frac{-Dx+mx(S^0-x)}{q(x)+mx}$ provides an explicit expression for the prey nullcline.

Chapter 3

Isocline Analysis

The equation of the prey nullcline is $F(x) = \frac{-Dx+mx(S^0-x)}{q(x)+mx}$. Some key properties of this function need to be established for use in later analysis. First note that $F(x)$ is continuously differentiable for $x \geq 0$. Continuity of $F(x)$ and $F'(x)$ is clear for $x > 0$. To obtain continuity at $x = 0$ L'Hopital's rule can be applied. Define the x-intercept of $F(x)$ by K such that $F(K) = 0$. Then $K = \frac{S^0 m - D}{m}$. The prey nullcline can be rewritten in terms of K as,

$$F(x; K) = \frac{mx(K-x)}{q(x)+mx}. \tag{3.1}$$

Since biologically relevant solutions are required, we must have $K > 0$, implying that $S^0 m - D > 0$.

3.1 Initial and End Behaviour

In order to determine the behaviour of the function $F(x; K)$, first examine its possible configurations at $x = 0$. There is a removable singularity at $x = 0$ since both numerator and denominator are zero there. Also, the y-intercept is always biologically relevant since

$$F(0) \triangleq \lim_{x \to 0} F(x) = \frac{Km}{m+1} > 0. \tag{3.2}$$

The initial behaviour of the prey nullcline is determined by the signs of $F'(0)$ and $F''(0)$. For the Ivlev response,

$$F'(0) \triangleq \lim_{x\to 0} F'(x) = \frac{m\,(K-2(m+1))}{2(m+1)^2} \tag{3.3}$$

$$\begin{cases} > 0 \text{ if } K > 2(m+1) \\ \leq 0 \text{ if } K \leq 2(m+1). \end{cases}$$

Similarly for $F''(0)$,

$$F''(0) \triangleq \lim_{x\to 0} F''(x) = \frac{-m\,(K(2m-1)+6(m+1))}{6(m+1)^3} \tag{3.4}$$

$$\begin{cases} > 0 \text{ if } K(2m-1)+6(m+1) < 0 \\ \leq 0 \text{ if } K(2m-1)+6(m+1) \geq 0. \end{cases}$$

If $m \geq \frac{1}{2}$, then $F''(0) < 0$ always. If $m < \frac{1}{2}$, $F''(0)$ can take on either sign. In other words, $m < 1/2$ is a necessary but not a sufficient condition for F to be concave up at $x = 0$. In order to guarantee that F is concave up initially, we need to satisfy $K(2m-1)+6(m+1) < 0$.

Proposition 3.1. *When the prey nullcline is initially concave up, it is also increasing.*

Proof. If $F''(0) > 0$,

$$\begin{aligned} 6(m+1) &< K(1-2m) \\ 2(m+1) &< \frac{K}{3}(1-2m) \\ &< \frac{K}{3} \text{ since } m < \frac{1}{2} \\ &< K. \end{aligned}$$

Therefore, if $F''(0) > 0$ then $F'(0) > 0$ necessarily. □

Now consider the end behaviour of F at $x = K$,

$$F'(K) = \frac{-mK}{mK + q(K)} < 0. \tag{3.5}$$

Thus $F(x)$ is always decreasing at $x = K$. Similarly, $F(x)$ is always concave down at $x = K$, since

$$F''(K) = \frac{2m(Ke^{-K} + e^{-K} - 1)}{(Km + 1 - e^{-K})^2} < 0 \text{ for } K > 0. \tag{3.6}$$

3.2 Location and Uniqueness of Extrema

Lemma 3.2. *If an interior local maximum of $F(x)$ exists, then it is located in the interval $(0, K/2)$.*

Proof. Factor the first derivative of $F(x)$ as follows:

$$F'(x) = \frac{m}{(mx + q(x))^2}[(K - 2x)(mx + q(x)) - x(K - x)(m + q'(x))]. \quad (3.7)$$

Since $mx + q(x) > 0$ and $m + q'(x) > 0$ for $x > 0$, we have that $F'(x) < 0$ for $\frac{K}{2} \leq x \leq K$. Therefore, if a local extrema exists, it must be located in $(0, K/2)$. □

Lemma 3.3. *The prey nullcline with Ivlev functional response has a unique maximum on $[0, K]$.*

Proof. Define M such that $F(M) = \max_{x\in[0,K]} F(x)$. Then,

$$\begin{aligned} F'(x) &= \frac{m}{(mx + 1 - e^{-x})^2}[(K - 2x)(mx + 1 - e^{-x}) - x(K - x)(m + e^{-x})] \\ &= \frac{m}{(mx + 1 - e^{-x})^2}[(K - 2x) - (e^{-x}(K + (K - 2)x - x^2) + mx^2)] \\ &= \frac{m}{(mx + 1 - e^{-x})^2}[k(x) - h(x)], \end{aligned}$$

where $k(x) = K - 2x$ and $h(x) = e^{-x}(K + (K - 2)x - x^2) + mx^2$. Consider the properties of $k(x)$ and $h(x)$.

$$\begin{array}{rclcrcl} k(0) &=& K & & h(0) &=& K \\ k'(0) &=& -2 & & h'(0) &=& -2 \\ k\left(\frac{K}{2}\right) &=& 0 & & h\left(\frac{K}{2}\right) &=& \frac{K^2}{4}(e^{-K/2} + m) > 0 \\ k'(x) &=& -2 & & h'(x) &=& e^{-x}(x^2 - Kx - 2) + 2mx. \end{array}$$

There are two cases to explore: $K \leq 2(m + 1)$ and $K > 2(m + 1)$.

First, if $K \leq 2(m + 1)$ then $F(x)$ is decreasing initially. Now look at the behaviour of $h''(x)$.

$$\begin{aligned} h''(0) &= 2(m + 1) - K \\ h''(x) &= e^{-x}(-x^2 + (K + 2)x + (2 - K)) + 2m \\ &= H(x)e^{-x} + 2m, \end{aligned} \quad (3.8)$$

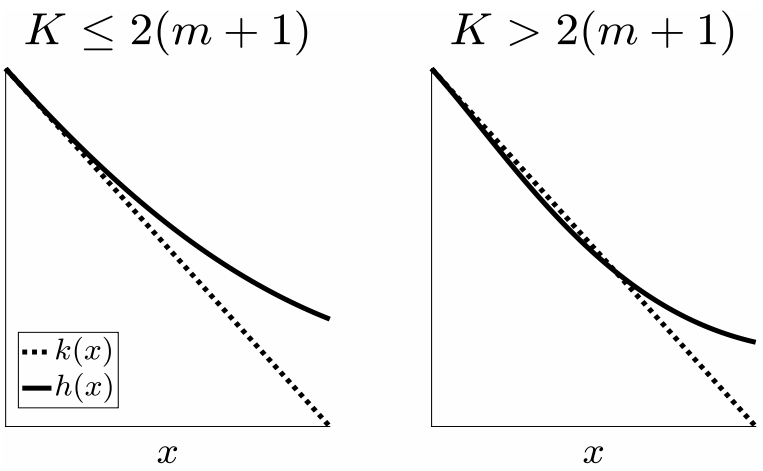

Figure 3.1: *The two cases for the functions $k(x)$ and $h(x)$ depending on the initial state of the nullcline. Parameters chosen were $D = 0.8$, $m = 0.1$, and K changed from 1.5 in the first plot to 4 in the second. When $F(x)$ is initially increasing, k and h intersect exactly once, leading to a unique local maximum of the prey nullcline.*

where $H(x) = -x^2 + (K+2)x + (2-K)$. Since $H(x)$ is a downward facing parabola with vertex at $x = 1 + K/2$, $H(x)$ is increasing over the interval $(0, K/2)$. Thus $h''(x) > 0$ implies $h'(x) > k'(x)$ on $(0, K/2)$ so there are no intersections of $k(x)$ and $h(x)$ on the interval. Therefore if $K \leq 2(m+1)$, $F(x)$ has no critical points and is decreasing over the interval $(0, K]$. In this case the unique maximum is $M = F(0)$.

In the case $K > 2(m+1)$, then $F(x)$ is increasing initially. Since $h''(0) < 0$, $h(K/2) > 0$, and $k(K/2) = 0$ there must be at least one intersection of $k(x)$ and $h(x)$ in $(0, K/2)$. Also since $H(x)$ is increasing over the interval $(0, K/2)$ it can change signs at most once. In turn $h''(x)$ must change signs exactly once. Therefore, since $h(x)$ starts concave down and below $k(x)$, ends concave up above $k(x)$, and must have exactly one inflection point, there is exactly one intersection of $k(x)$ and $h(x)$ in $(0, K/2)$. Thus $F(x)$ has a unique local maximum M in $(0, K/2)$ when $K > 2(m+1)$. □

Lemma 3.4. *If $F''(0) \geq 0$, then $F(x)$ has a unique inflection point in $[0, M)$ and no inflection points in $[M, K]$. If $F''(0) < 0$, then $F(x)$ is strictly concave down on $[0, K]$.*

Proof. For the case $F''(0) \geq 0$, start by noticing that $F''(x)$ is linear in K.

Solve the equation $F''(x) = 0$ for K, and denote this special value of K by $\tilde{K}$.

$$\tilde{K}(x) = \frac{2 + (x^2 + 4\,x + 2)\,e^{-2x} + (mx^3 + x^2 - 4\,x - 4)\,e^{-x}}{(x+2)\,e^{-2x} + (mx^2 + (2\,m+1)\,x + 2\,m - 2)\,e^{-x} - 2\,m} \tag{3.9}$$

Taking the derivative of $\tilde{K}$ with respect to x yields:

$$\tilde{K}'(x) = \frac{e^{-x}\,(mx + 1 - e^{-x})^2\,((x^2 + 4\,x + 6)\,e^{-x} + 2\,x - 6)}{((x+2)\,e^{-2x} + (mx^2 + (2\,m+1)\,x + 2\,m - 2)\,e^{-x} - 2\,m)^2}.$$

The sign of $\tilde{K}'(x)$ is determined by the sign of $(x^2 + 4\,x + 6)\,e^{-x} + 2\,x - 6$. This function and its first derivative are both zero at $x = 0$ and its second derivative is $x^2e^{-x} \geq 0$ for $x \geq 0$. Thus $(x^2 + 4x + 6)\,e^{-x} + 2x - 6 \geq 0$ for $x \geq 0$, so $\tilde{K}(x)$ is an increasing function with respect to x. Now study the denominator of $\tilde{K}(x)$, denoted here by $d(x)$:

$$\begin{aligned}
d(x) &= (x+2)e^{-2x} + ((x^2 + 2x + 2)m + x - 2)e^{-x} - 2m \\
d'(x) &= e^{-x}(3(1 - e^{-x}) - x(2e^{-x} + mx + 1)) \\
d(0) &= 0,\ d'(0) = 0,\ d''(0) = 0,\ \text{and } d'''(0) = 1 - 2m \\
\lim_{x\to\infty} d(x) &= -2m.
\end{aligned}$$

We now show that for $m < 1/2$, $d(x)$ has a unique root, and for $m \geq 1/2$, $d(x)$ has no positive roots. Let $h(x) = 3(1-e^{-x})$ and $k(x) = x(2e^{-x}+mx+1)$. Then $d(x) = e^{-x}(h(x) - k(x))$. Consider the properties of the continuous functions $h(x)$ and $k(x)$:

$$\begin{array}{rclcrcl}
h(0) &=& 0 & & h(0) &=& K \\
h'(0) &=& 3 & & k'(0) &=& 3 \\
h''(0) &=& -3 & & k''(0) &=& -4 + 2m \\
\lim\limits_{x\to\infty} h(x) &=& 3 & & \lim\limits_{x\to\infty} k(x) &=& \infty.
\end{array}$$

It is also clear that $h(x)$ is increasing and concave down for $x > 0$. Also important to note is that $k(x)$ is increasing for $x > 0$. To see this, consider $k(x; m)$. The first derivative of $k(x; m)$ is an increasing function of m for $x > 0$. Thus,

$$0 < 2(1 - x)e^{-x} + 1 = k'(x; m = 0) < k'(x; m > 0). \tag{3.10}$$

As such, $k(x; m)$ is strictly increasing for $x > 0$ and $m > 0$. Based on the initial and ending configurations for $h(x)$ and $k(x)$, and the fact that both functions are strictly increasing, if $m < 1/2$, then $k(x)$ intersects $h(x)$ exactly once for $x > 0$. Thus $\tilde{K}(x)$ has one vertical asymptote for $x > 0$. If $m \geq 1/2$ then

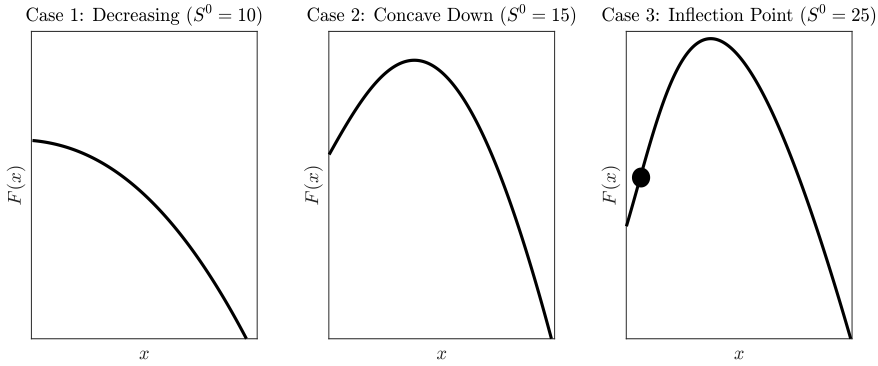

Figure 3.2: *The three possible isocline configurations with Ivlev response for parameters $m = 0.1$, $D = 0.8$. S^0 is varied. Plotted using Matlab [24]. The dot on the right plot shows the location of the inflection point.*

$h(x)$ and $k(x)$ have no positive intersections, so $\tilde{K}(x)$ is continuous. Finally, looking at the initial and ending behaviour of $\tilde{K}(x)$ determines its possible configurations when $x > 0$.

$$\lim_{x\to 0} \tilde{K}(x) = \frac{-6(m+1)}{2m-1}$$

Also,

$$\lim_{x\to \infty} \tilde{K}(x) = \frac{-1}{m}. \tag{3.11}$$

When $m < 1/2$, $\tilde{K}$ is initially positive, and when $m > 1/2$ it is initially negative. Based on this we can conclude that for $m \geq 1/2$, $\tilde{K}(x) < 0$ for $x > 0$. Thus, $F''(x)$ cannot change signs for any value of $K > 0$, so $F(x)$ has no inflection points in $[0, K]$. When $m < 1/2$, $F''(x)$ can change signs at most once for a particular value of K, so $F(x)$ has at most one inflection point in this case. □

We can therefore conclude that there are only 3 biologically relevant configurations of the prey nullcline with Ivlev response to consider, as shown in Figure 3.2. In the first two cases $F(x)$ is concave down for x in $[0, K]$. In the third case $F(x)$ is initially concave up, then becomes concave down.

It is also relevant to determine how the local maximum of $F(x)$ moves as the parameter S^0 is varied. Consider the partial derivative of the prey nullcline

with respect to K.

$$\frac{\partial F}{\partial K} = \frac{mx}{mx + q(x)} > 0 \tag{3.12}$$

Since $\frac{\partial F}{\partial K} > 0$ for $x > 0$, as K is increased the maximum moves up. Next consider $\frac{\partial^2 F}{\partial K \partial x}$ given by:

$$\frac{\partial^2 F}{\partial K \partial x} = \frac{m(q(x) - xq'(x))}{(mx + q(x))^2}. \tag{3.13}$$

The denominator of (3.13) is clearly always positive, so examine the numerator. For the Ivlev response, $q(x) - xq'(x) = 1 - xe^{-x} - e^{-x}$. This function is zero at $x = 0$ and increasing for $x > 0$, so $q(x) - xq'(x) > 0$. Thus $\frac{\partial^2 F}{\partial S^0 \partial x} > 0$, so the local maximum moves up and to the right as S^0 increases.

Remark. *For any $x^* > 0$ it is possible to find a critical value of K, denoted $\hat{K}$, such that $F'(x^*; \hat{K}) = 0$. Since $F'(x)$ is an increasing function of K, solve the expression $F'(x^*) = 0$ for K and denote it $\hat{K}$:*

$$\hat{K} = \frac{-\ln(1-D)\left[(D+m-1)\ln(1-D) - 2D\right]}{D\ln(1-D) - \ln(1-D) - D} \tag{3.14}$$

Then $F'(x^*; \hat{K}) = 0$ for any fixed $x^* > 0$.

Chapter 4

Stability Analysis

4.1 Fixed Points and Local Stability

There are three possible critical points of this system. The $(0,0)$ and $(K,0)$ equilibria always exist when $K > 0$. The coexistence equilibrium is given by (x^*, y^*), where $x^* = q^{-1}(D)$ and $y^* = F(x^*)$. Recall for the Ivlev response that $x^* = -\ln(1-D)$. Since $0 < D < 1$ and $F(x) > 0$ for $0 \leq x < K$, we have $y^* > 0$. Thus the interior equilibrium point will exist if and only if $x^* < K$. Refer to table 4.1 for a summary of the equilibrium points and their existence criteria. We now consider the local stability for these fixed points.

The Jacobian matrix for system (2.8) is given by:

$$J(x,y) = \begin{bmatrix} -(q'(x)+m)(y-F(x)) + (q(x)+mx)F'(x) & -q(x)-mx \\ yq'(x) & -D+q(x) \end{bmatrix}. \tag{4.1}$$

Equilibrium Point	**Existence Criteria**
$(0,0)$	Always exists
$(K,0)$	$K > 0$
$(x^*, y^*) = (q^{-1}(D), F(q^{-1}(D)))$	$K > 0$, and $q^{-1}(D) < K$

Table 4.1: *The three equilibrium points of system (2.8), along with the criteria under which they exist.*

Evaluating at the zero equilibrium we obtain:

$$J(0,0) = \begin{bmatrix} (q'(0)+m)F(0) & 0 \\ 0 & -D \end{bmatrix}. \tag{4.2}$$

Recall from the properties of $q(x)$ that $q'(x) \geq 0$ for $x \geq 0$. Hence the origin is a saddle point since the diagonal entries have opposite signs.

Performing the same analysis on $(K, 0)$,

$$J(K,0) = \begin{bmatrix} (q(K)+mK)F'(K) & -q(K)-mK \\ 0 & -D+q(K) \end{bmatrix}. \tag{4.3}$$

If $x^* > K$, i.e. no interior equilibrium point exists, $-D + q(K) = -q(x^*) + q(K) < 0$ and $F'(K) < 0$ so $(K, 0)$ is locally stable. To guarantee the existence of a coexistence equilibrium, however, we require $x^* < K$. In this case, the diagonal entries of $J(K, 0)$ have opposite signs and $(K, 0)$ is a saddle point.

Lastly we consider the coexistence equilibrium which exists under the condition $x^* < K$:

$$J(x^*,y^*) = \begin{bmatrix} (mx^*+D)F'(x^*) & -(mx^*+D) \\ y^*q'(x^*) & 0 \end{bmatrix}. \tag{4.4}$$

The characteristic equation is:

$$0 = \lambda^2 - \lambda(mx^*+D)F'(x^*) + (mx^*+D)y^*q'(x^*). \tag{4.5}$$

We know $mx^* + D > 0$, $y^* > 0$ and $q'(x^*) > 0$, so the constant term of the characteristic equation is positive. The roots of (4.5) have negative real part if and only if $F'(x^*) < 0$. As such, (x^*, y^*) is locally stable when $F'(x^*) < 0$ and is unstable when $F'(x^*) > 0$. If $F'(x^*) = 0$ or $x^* = K$ then the equilibrium point is non-hyperbolic. In Chapter 6 it is determined that a supercritical Hopf bifurcation occurs at $F'(x^*) = 0$, so the coexistence equilibrium is asymptotically stable there. It follows from standard phase plane analysis that (x^*, y^*) is asymptotically stable when $x^* = K$.

4.2 Global Stability

Some asymptotic properties of this chemostat system can be established using a Lyapunov function. As in Harrison [10], a Lyapunov function for system

(2.8) is given by

$$V(x,y) = \int_{x*}^{x} \frac{q(z)-D}{q(z)+mz}dz + \int_{y^*}^{y} \frac{z-y^*}{z}dz \tag{4.6}$$
$$= \int_{x*}^{x} \frac{(1-e^{-z})-D}{(1-e^{-z})+mz}dz + y - y^* + y^* \ln\left(\frac{y^*}{y}\right)$$

It is clear that $V(x^*, y^*) = 0$. Also, since $q(x)$ is an increasing function, $\frac{q(z)-q(x^*)}{q(z)+mz}$ has the same sign as $x - x^*$, and $\frac{z-y^*}{z}$ has the same sign as $y - y^*$. Thus $V(x, y) > 0$ for $(x, y) \neq (x^*, y^*)$. We also have

$$\dot{V}(x,y) = (q(x) - q(x^*))(F(x) - F(x^*)) \tag{4.7}$$

The sign of $\dot{V}$ is dependent on the location of the vertical isocline with respect to the local maximum. If $F'(0) \leq 0$, then $F(x)$ is a decreasing function and so $F(x) - F(x^*) > 0$ for $x < x^*$, and $F(x) - F(x^*) < 0$ for $x > x^*$. Since $q'(x) > 0$, $q(x) - q(x^*) < 0$ for $x < x^*$ and $q(x) - q(x^*) > 0$ for $x > x^*$. In both cases $x < x^*$ and $x > x^*$, we have $\dot{V} \leq 0$, with equality if and only if $x = x^*$, so the interior equilibrium point is stable. Now consider the case $F'(0) > 0$ so that the prey nullcline has a local maximum in the first quadrant. Define as usual $M > 0$ as the unique point such that $F'(M) = 0$. Then since $F'(x) < 0$ for $M < x < K$, there exists a unique point $\xi \in (M, K)$ such that $F(\xi) = F(0)$. Taking $x^* > \xi$ and applying this Lyapunov function the local stability of (x^*, y^*) for $x^* \in (\xi, K)$ is obtained.

The local stability results from Harrison's Lyapunov function can be extended to global asymptotic stability on this region using the LaSalle extension theorem [19].

Lemma 4.1. *Let $\mathcal{E} = \{(x, y) : \dot{V}(x, y) = 0\}$, and let $\mathcal{M}$ be the largest invariant subset of $\mathcal{E}$. Then $\mathcal{M} = \{(x^*, y^*)\}$.*

Proof. For system (2.8) the set $\mathcal{E} = \{(x, y) : x = x^*, y \geq 0\}$. Thus for the solution to be in $\mathcal{M}$ for all $t \geq 0$ we have $x(t) = x^*$ $\forall t \geq 0$. Since the x value is fixed at x^* we have $x'(t) = (mx^* + q(x^*))(F(x^*) - y) = 0$ with initial condition $x(0) = x^*$. This condition is satisfied only if $F(x^*) = y$, i.e. if $y(t) = y^*$ $\forall t \geq 0$. □

By Lemma 2.1 all orbits of system (2.8) are bounded. Since the largest invariant set only consists of the coexistence equilibrium point, every bounded orbit must converge to it and as such (x^*, y^*) is globally asymptotically stable.

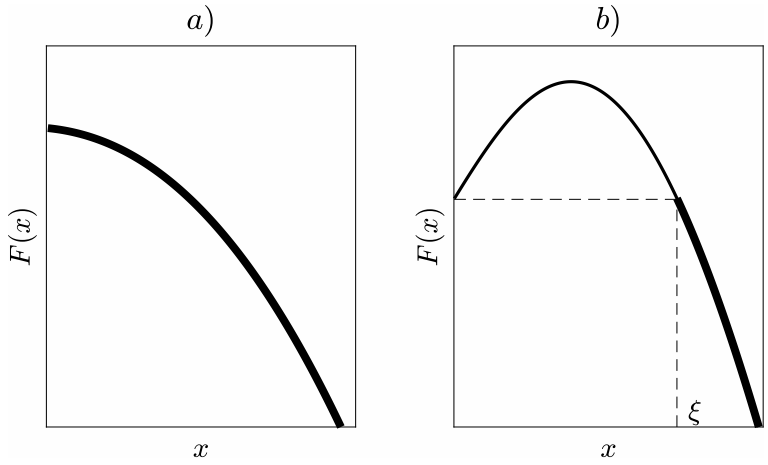

Figure 4.1: *If x^* intersects the bold region of the nullcline $F(x)$, then global stability of the coexistence equilibrium has been established using the Lyapunov function in (4.6). In plot a) we can see that since the isocline has no local extrema, the Lyapunov function gives global asymptotic stability on the entire downward slope. In plot b) the isocline is initially increasing so global stability is only obtained for $x^* > \xi$ using this method.*

The position of the coexistence equilibrium on the prey nullcline where its global asymptotic stability can be established using the Lyapunov function defined in (4.6) and the LaSalle Extension Theorem can be seen in Figure 4.1.

We conjecture that whenever the coexistence equilibrium point is locally asymptotically stable, it is globally asymptotically stable. In other words, (x^*, y^*) is a global attractor for $M \leq x^* \leq K$. It is proved in Chapter 6 that there is a supercritical Hopf bifurcation at $x^* = M$ so the equilibrium point is locally asymptotically stable there. Here we take an approach similar to that of Hsu, who hypothesized in Theorem 3.3 of [13] that the coexistence equilibrium is globally asymptotically stable whenever the prey nullcline is concave down. This was later proved to be incorrect and a counterexample was provided by Hofbauer and So in [11]. Here we follow the initial approach from [13] by applying the Dulac criterion with $h(x) = (q(x) + mx)^{-1} y^{\beta-1}$ as the auxiliary function. The constant $\beta > 0$ here is to be determined. Note that $h(x, y)$ is defined in the interior of quadrant one. Also let $f = \begin{pmatrix} x' \\ y' \end{pmatrix}$.

Then the divergence of the vector field is given by:

$$\Delta \triangleq \nabla \cdot (hf) = \frac{y^{\beta-1}H(x)}{q(x)+mx} \tag{4.8}$$

where $H(x) = (q(x)+mx)F'(x) + \beta(q(x)-D)$. In the interior of the positive quadrant we have $q(x)+mx > 0$ and $y^{\beta-1} > 0$ implying that Δ changes sign if and only if $H(x)$ changes sign. This is where we must diverge from Hsu's Theorem 3.3. We use the facts that on $[0, M]$, $F'(x) \geq 0$ and $q(x) - D < 0$, and for $x \in [x^*, K]$, $q(x) - D > 0$. Ultimately it is our choice of β that is critical in determining that $H(x)$ does not change sign. For $x \in [M, x^*]$ both $F'(x) \leq 0$ and $q(x) - D \leq 0$, so for any $\beta > 0$ we have $H(x) \leq 0$. The regions $0 \leq x < M$ and $x^* < x \leq K$ pose more of a challenge.

Let $\beta(x) = \frac{-F'(x)(mx+q(x))}{q(x)-D}$. In order to ensure that $H(x)$ does not change signs we need to find a value $\beta > 0$ such that $\max\limits_{x\in[0,M]} \beta(x) < \beta < \min\limits_{x\in[x^*,K]} \beta(x)$.

$$\beta(x;K) = \frac{-F'(x)(mx+q(x))}{q(x)-D} \tag{4.9}$$

$$= \frac{m\left(x\left(K-x\right)q'(x) + \left(2x-K\right)q\left(x\right) + mx^2\right)}{\left(mx+q\left(x\right)\right)\left(q\left(x\right)-D\right)}. \tag{4.10}$$

Now differentiate β with respect to the parameter K:

$$\frac{\partial}{\partial K}\beta(x;K) = \frac{m(xq'(x)-q(x))}{(mx+q(x))(q(x)-D)}. \tag{4.11}$$

To understand the sign of this derivative first note that $xq'(x) - q(x) = xe^{-x} + e^{-x} - 1 < 0 \; \forall \; x > 0$. Then, $\beta(x)$ is an increasing function of K if $x < x^*$ and a decreasing function of K if $x > x^*$. Taking $K = \hat{K}$ from (3.14) forces $x^* = M$. Since $x^* > M$ originally, forcing $x^* = M$ causes the local maximum to move up and to the right by (3.13). To maintain $x^* > M$ we must therefore have $K < \hat{K}$. Let

$$\hat{\beta}(x) \triangleq \beta(x;\hat{K}), \tag{4.12}$$

and

$$\hat{\beta}_{\text{crit}} \triangleq \lim_{x\to x^*} \hat{\beta}(x)$$

$$= \frac{m\left[(D-1)\ln^2(1-D) - 2\nu(D)\right]}{(D-1)\nu(D)}, \tag{4.13}$$

where $\nu(D) = (D-1)\ln(1-D) - D$. To establish the sign of $\hat{\beta}_{\text{crit}}$, we examine the properties of $\nu(D)$. We have

$$\begin{aligned} \nu(D) &= (D-1)\ln(1-D) - D \\ \nu(0) &= 0 \\ \nu'(D) &= \ln(1-D) < 0 \quad \forall\ 0 < D < 1. \end{aligned} \tag{4.14}$$

Thus $\nu(D)$ is negative for $0 < D < 1$ and so $\hat{\beta}_{\text{crit}} > 0$.

Theorem 4.2. *If (x^*, y^*) is a locally asymptotically stable equilibrium point of system (2.8) with Ivlev functional response and $\hat{\beta}(x)$ from (4.12) is an increasing function of x, then (x^*, y^*) is globally asymptotically stable.*

Proof. The function $\hat{\beta}(x) = \beta(x; \hat{K})$ is defined in (4.12), where $\hat{K}$ is as in (3.14). If $\hat{\beta}(x)$ is an increasing function of x and $x < M$, then we have $\beta(x; K) < \hat{\beta}(x) < \hat{\beta}_{\text{crit}}$, where $\hat{\beta}_{\text{crit}}$ is as defined in (4.13). In the case $x > x^*$, we similarly have $\hat{\beta}_{\text{crit}} < \hat{\beta}(x) < \beta(x; K)$. It remains to test the boundaries,

$$\beta(M; S^0) = 0 < \hat{\beta}_{\text{crit}} \tag{4.15}$$

and

$$\lim_{x \to x^{*+}} \beta(x; S^0) = \infty > \hat{\beta}_{\text{crit}}. \tag{4.16}$$

Finally we have

$$\max_{x \in [0, M]} \beta(x; K) < \hat{\beta}_{\text{crit}} < \min_{x \in [x^*, K]} \beta(x; K). \tag{4.17}$$

As such, $\hat{\beta}_{\text{crit}}$ is the exact value of β needed for the Dulac criterion in (4.8). With this β we ensure that $H(x)$ does not change sign in the region and hence, by the Dulac criterion, there are no closed periodic solutions lying entirely in the region. Since in addition all orbits are bounded, the Poincaré-Bendixson theorem implies that the interior equilibrium must be globally asymptotically stable with respect to initial conditions in the interior of the first quadrant. □

Remark. *The result that local stability implies global stability as stated above requires that $\hat{\beta}(x)$ is an increasing function of x. In order for this global stability result to be rigorous an additional proof that $\hat{\beta}'(x) > 0$ is required. We conjecture that for the Ivlev functional response this is the case and an example is provided in Figure 4.2. Also note that this condition will be required again in Theorem 5.3. As such, it is an important open problem.*

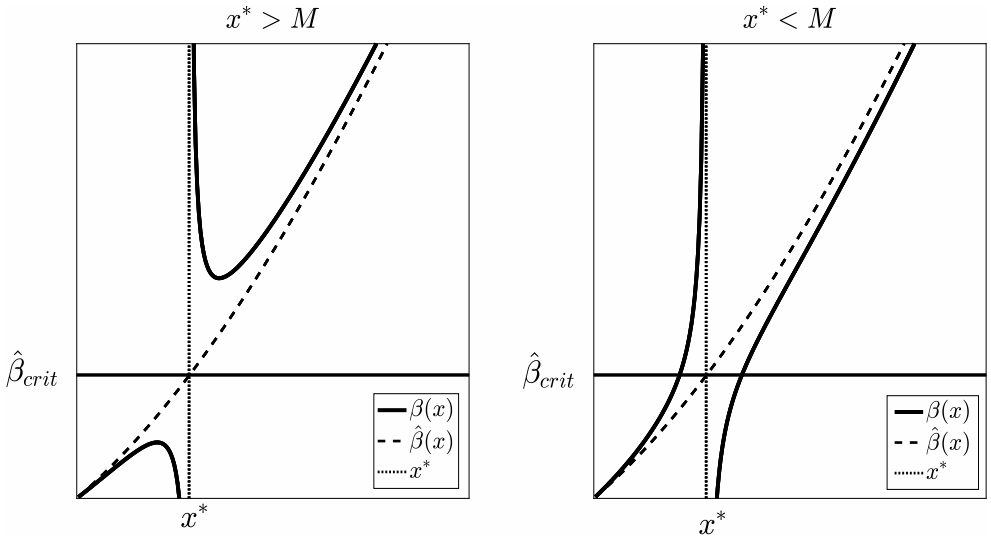

Figure 4.2: *An example where an appropriate β can be found for the Dulac function in (4.8). In this case, with $D = 0.5$ and $m = 0.25$ we can find the $\hat{\beta}_{crit}$ when $K < \hat{K}$ ($x^* > M$), but not when $K > \hat{K}$ ($x^* < M$). This gives global stability of the coexistence equilibrium whenever $F'(x^*) < 0$.*

Chapter 5

Periodic Orbits

It has been established via the global attractivity argument that system (2.8) has no periodic orbits when $F'(x^*) < 0$. We now prove that when periodic orbits do exist, they must surround the local maximum at $(M, F(M))$.

Lemma 5.1. *Let Γ be any periodic orbit of system (2.8). Then,*

$$\Delta \triangleq \oint_\Gamma \nabla \cdot (\dot{x}, \dot{y}) dt = \oint_\Gamma (mx + q(x))F'(x)dt.$$

Proof. Let $g(x) = -D + m(S^0 - x)$ and $l(x) = mx + q(x)$. Then $\dot{x} = xg(x) - yl(x)$ and the integral becomes

$$\begin{aligned}
\Delta &= \oint_\Gamma \left[(xg'(x) + g(x) - y(q'(x) + m)) + (-D + q(x))\right] dt \\
&= \oint_\Gamma \left[xg'(x) + g(x) + \left(\frac{\dot{x} - xg(x)}{l(x)}\right) l'(x) + \frac{\dot{y}}{y}\right] dt \\
&= \oint_\Gamma \left[\frac{l(x)(xg'(x) + g(x)) - xg(x)l'(x)}{l(x)} + \left(\frac{\dot{x}}{l(x)}\right) l'(x) + \frac{\dot{y}}{y}\right] dt \\
&= \oint_\Gamma \left[l(x)F'(x) + \dot{x}\frac{l'(x)}{l(x)} + \frac{\dot{y}}{y}\right] dt \\
&= \oint_\Gamma \left[l(x)F'(x) + \frac{d}{dt}\ln\left(l(x)\right) + \frac{d}{dt}\ln\left(y\right)\right] dt \\
&= \oint_\Gamma (mx + q(x))F'(x)dt.
\end{aligned}$$

□

Since $mx + q(x) > 0$, the sign of Δ depends on the sign of $F'(x)$. By the Poincaré criterion [5], if $\Delta > 0$, then the periodic orbit is unstable and if $\Delta < 0$, any periodic orbit is stable.

Proposition 5.2. *Any periodic orbit of (2.8) must surround the point* $(M, F(M))$.

Proof. Suppose that $F'(x) > 0$ for the entire portion of $F(x)$ that lies inside Γ. Then by Lemma 5.1, $\Delta > 0$, so by the Poincaré criterion Γ must be an unstable periodic orbit. Also, Γ must surround the coexistence equilibrium at (x^*, y^*), implying that $F'(x^*) > 0$ so the equilibrium point is unstable. This is a contradiction since we cannot have an unstable periodic orbit surrounding an unstable equilibrium point.

Now suppose $F'(x) < 0$ for the entire portion of $F(x)$ that lies inside Γ. Then $\Delta < 0$ so Γ must be a stable periodic orbit. The coexistence equilibrium is locally stable when $F'(x^*) < 0$. Thus we have a contradiction since we cannot have only stable periodic orbits surrounding a stable equilibrium point.

Therefore the slope of the portion of $F(x)$ that lies inside of any periodic orbit cannot be entirely of one sign. Finally, since the critical point at $(M, F(M))$ is unique, the only way for $F'(x)$ to change sign is for Γ to surround this local maximum. □

5.1 Uniqueness of the Periodic Orbit

In 1987, Zhang proved the uniqueness of the periodic orbit for generalized Liénard equations [32]. A Liénard equation has the form:

$$\frac{d^2x}{dt^2} + f(x)\frac{dx}{dt} + g(x) = 0,$$

where $f, g \in C^1(\mathbb{R})$, f is an even function, and g is an odd function [20]. Zhang's result is well used in the study of quadratic ordinary differential systems, including the classical predator-prey model. In 1988 Zhang's theorem was extended by Huang to encompass a wider variety of predator-prey models, including Lotka-Volterra, Gause-type and others [14]. Here, we use a slightly adapted version of Huang's theorem that better applies to our system. This adapted version accounts for the invariance of system (2.8) in the first quad-

rant. We consider systems of the form:

$$\begin{aligned} \frac{dx}{dt} &= \phi(x)\left(F(x) - \pi(y)\right), \\ \frac{dy}{dt} &= \rho(y)\psi(x). \end{aligned} \tag{5.1}$$

Theorem 5.3. *(Theorem 1 from [14]) Consider system (5.1). If*

(i) $\exists\ K > x^*$ *such that* $F(K) = 0$ *and* $(x-K)F(x) < 0$ *for* $x \neq K$, $\exists\ 0 < x^* < K$ *such that* $\psi(x^*) = 0$, *i.e. there is a positive equilibrium point* (x^*, y^*),

(ii) all functions in (5.1) are C^1 *in the interior of* $\mathbb{R}^3_+$, *and* $F'(x)$ *is continuous in the interior of* $\mathbb{R}^3_+$,

(iii) $\phi(0) = \pi(0) = \rho(0) = 0$, $\phi'(x) > 0$ *and* $\psi'(x) > 0$ *for* $x > 0$, $\rho'(y) > 0$ *and* $\pi'(y) > 0$ *for* $y > 0$, *and*

(iv) $H(x) = -F'(x)\phi(x)/\psi(x)$ *is non-decreasing for* $0 < x < x^*$ *and* $x^* < x < K$.

Then, system (5.1) has at most one limit cycle in the first quadrant, and if it exists it is stable.

The uniqueness result from Huang's theorem follows by making a change of variables and applying Zhang's Theorem [32].

For the chemostat system in (2.8) with Ivlev response, take $\phi(x) = mx + q(x)$, $\pi(y) = \rho(y) = y$ and $\psi(x) = q(x) - D$ to obtain the same form as (5.1). Conditions (i), (ii) and (iii) are easily verified, leaving only condition (iv). Recall from the previous chapter that this function $H(x)$ is exactly the same as $\beta(x)$ from (4.9), which was used to establish the global stability of (x^*, y^*) when $x^* > M$. Also, Theorem 4.2 required $\hat{\beta}'(x) > 0$. This condition is equivalent to condition (iv) above since for periodic orbits we need $K > \hat{K}$ from (3.14) to ensure $x^* < M$. This implies that uniqueness of the periodic orbit follows as a corollary from Theorem 4.2, so when the equilibrium point falls to the right of the maximum it is globally asymptotically stable, and when it falls to the left there is a unique periodic orbit. The non-decreasing nature of $H(x)$ has been observed in all of the examples we considered. One such example is given in Figure 4.2, with $m = 0.25$ and $D = 0.5$. In this figure, the non-decreasing nature of $H(x)$ can be visually observed when $x^* < M$. This proof has not been completed in general for the Ivlev response function. A proof that the periodic orbit is unique for all choice of parameters such that x^* is to the left of the local maximum of the prey nullcline is given in Chapter 8 for the Monod functional response.

For Ivlev functional response specifically, uniqueness of the periodic orbit was established for the classical predator-prey model by Kooij and Zegeling [17]. For the chemostat model, the analogous approach of transformation to a Liénard system can be applied. To do so, the preliminary theorems from Zhang [32] and accompanying lemmas from [17] need to be restated.

Theorem 5.4. *(Theorem 1.1 from [17]) Let $f(x)$ and $g(x)$ be continuously differentiable functions on an open interval (r_1, r_2), and let $\Psi(y)$ by continuously differentiable on $\mathbb{R}$. Consider:*

$$\begin{aligned} \frac{dx}{dt} &= \Psi(y) - \int_{x_0}^{x} f(\tau)d\tau, \\ \frac{dy}{dt} &= -g(x). \end{aligned} \tag{5.2}$$

such that:
(i) $\frac{d\Psi(y)}{dy} > 0$,
(ii) $x_0 \in (r_1, r_2)$ *is the unique value such that* $(x - x_0)g(x) > 0$ *for* $x \neq x_0$ *and* $g(x_0) = 0$, *and*
(iii) $f(x_0)\frac{d}{dx}(\frac{f(x)}{g(x)}) < 0$ *for* $x \neq x_0$.
Then, system 5.2 has at most one limit cycle, and if it exists, it is hyperbolic.

Since we are considering a parameter dependent system, Theorem 5.4 can be used in combination with the Dulac function $B(x, y) = e^{-cy}$ from [18] to obtain information over the entire parameter space. This leads to a modified version of Theorem 5.4 that is useful since it can be interpreted graphically.

Theorem 5.5. *(Theorem 1.2 from [17]) Suppose a Liénard system (5.2) satisfies the following on $r_1 < x < r_2$:*
(i) and (ii) as in Theorem 5.4, and either:
(iii)′ $\exists\ c \in \mathbb{R}$, *such that* $f(x) - cg(x)$ *has no zeros, or*
(iii)″ $\forall\ c \in \mathbb{R}$, $f(x) - cg(x)$ *has no multiple zeros and* $f(x_0) \neq 0$.
Then, system (5.2) has at most one limit cycle and if it exists it is hyperbolic.

In the case of $(iii)'$, no intersection of $f(x)$ with $cg(x)$ implies that no limit cycle exists. In $(iii)''$, if for all choices of c, $f(x)$ has no tangency points with $cg(x)$, then there is at most one limit cycle. A proof of the equivalence of Theorems 5.4 and 5.5 is given in [18]. The following three lemmas from [17] are used to verify the conditions of Theorem 5.5.

Lemma 5.6. *(Lemma 1.3 from [17]) If $f(x)$ has exactly one zero at $x = x_1$ on the interval $r_1 < x < r_2$, then condition $(iii)''$ from Theorem 5.5 only needs to be satisfied on the intervals $r_1 < x < x_1$ and $x_0 < x < r_2$ if $x_1 < x_0$*

($r_1 < x < x_0$ and $x_1 < x < r_2$ if $x_0 < x_1$), in order to draw the same conclusions as Theorem 5.5.

Lemma 5.7. *(Lemma 1.4 from [17]) Define $f(x) = s(x)f_1(x)$ and $g(x) = s(x)g_1(x)$, where $s(x)$ is a positive, continuously differentiable function on (r_1, r_2). If $f_1(x)$ and $f_2(x)$ satisfy the conditions in Theorems 5.4 and 5.5, then so do $f(x)$ and $g(x)$.*

Lemma 5.8. *(Lemma 1.5 from [17]) If the conditions of Theorems 5.4 and 5.5 are met with $x = k(u)$, $dk/du \neq 0$, where all derivatives are taken wrt u instead of x, and all x-intervals are replaced by the corresponding interval in u, $k^{-1}(r_1) < u < k^{-1}(r_2)$, then system (5.2) has at most one limit cycle*

To prove uniqueness of the periodic orbit, the sequence of steps taken is to first transform system (2.8) into a Liénard system. Then, in accordance with Lemma 5.7, identify and remove the common factor $s(x)$ from $f(x)$ and $g(x)$ and continue the analysis using f_1 and g_1. Next, apply Lemma 5.8 to perform a change of variables $x = k(u)$, and finally attempt to prove that the functions $f^*(u) = f_1(k(u))$ and $g^*(u) = g_1(k(u))$ satisfy the conditions outlined in Theorem 5.5.

Making a change of variables similar to that of [17], $y \mapsto e^{y_1}$ and $t \mapsto -t_1/(mx + q(x))$, and restoring the original notation, system (2.8) becomes:

$$\begin{aligned} x' &= e^y - \frac{x(-D + m(S^0 - x))}{mx + q(x)} = e^y - F(x) \\ y' &= \frac{D - q(x)}{mx + q(x)} \end{aligned} \tag{5.3}$$

Transform to a Liénard system of the form of (5.2) by taking

$$\begin{aligned} \Psi(y) &= e^y - \frac{mx^*(K - x^*))}{mx^* + q(x^*)} = e^y - F(x^*) \\ f(x) &= F'(x) = s(x)f_1(x), \quad g(x) = s(x)g_1(x) \\ f_1(x) &= m(K - 2x) - \frac{mx(K - x)(m + q'(x))}{mx + q(x)} \\ g_1(x) &= -D + q(x) \\ s(x) &= \frac{1}{mx + q(x)}, \end{aligned} \tag{5.4}$$

where x_0 is the unique zero of $g(x)$ in the first quadrant. This zero is unique since the denominator of $g(x)$ is always positive in the interior of quadrant

one, so the only zero is located where $q(x) = D$. As such, x_0 corresponds with the coexistence equilibrium point so that $x_0 = x^* = -\ln(1 - D)$.

It remains to show that $f(x)$ and $g(x)$ satisfy the conditions of Theorem 5.5. Applying Lemma 5.7 this is equivalent to showing that $f_1(x)$ and $g_1(x)$ satisfy the criteria for a Liénard system. Condition (i) is trivial since $\frac{d\Psi}{dy} = e^y > 0$. For condition (ii) we need $x_0 \in (0, K)$ to be the unique value such that $(x - x_0)g(x) > 0$ for $x \neq x_0$, and $g(x_0) = 0$. This is the case since

$$\begin{aligned} g(x) &= \frac{-D + q(x)}{mx + q(x)}, \\ g(x_0) &= g(x^*) = 0, \\ (x - x_0)g(x) &= (x - x^*)g(x). \end{aligned}$$

If $x > x^*$, then $q(x) > D \implies (x - x^*)g(x) > 0$, and if $x < x^*$ then $q(x) < D \implies (x - x^*)g(x) > 0$. Therefore condition (ii) holds. It now remains to check $(iii)'$ and $(iii)''$. In accordance with Lemma 5.8 a change of variables $x = k(u) = -\ln(u)$ will be used. We choose this $k(u)$ so as to make $g^*(u)$ a decreasing linear function. Note that $d(k(u))/du < 0$, so now condition (ii) is not satisfied. This change of sign can be justified by making another change of variables $x \mapsto -x$ in (5.4) to ensure (ii) holds. The interval under consideration is $0 < x < K \implies e^{-K} < u < 1$. Therefore, taking $0 < u < 1$ is sufficient for the proof. Applying this change of variables to f_1 and g_1 gives:

$$\begin{aligned} g_1(x) &= -D + 1 - e^{-x} \\ g^*(u) &= g_1(k(u)) = -D + 1 - u \\ f_1(x) &= m(K - 2x) - \frac{mx(K - x)(m + e^{-x})}{mx + 1 - e^{-x}} \\ f^*(u) &= \frac{m(m - u)\ln^2(u) + m(Ku + 2(u - 1))\ln(u) + Km(u - 1)}{m\ln(u) + 1 - u}. \end{aligned} \tag{5.5}$$

We now need to prove that $\forall\ u \in (0, 1)$, either $f^*(u) - cg^*(u)$ has no zeros for a certain choice of c, or that it has no multiple zeros $\forall c \in \mathbb{R}$. First some properties of f^* and g^* are required. The root of g^* is at $u = 1 - D$, and since $0 < D < 1$, the root of g^* will always exist in the given interval.

Lemma 5.9. *If $F'(0) \leq 0$, then $f^*(u)$ has no zeros in $(0, 1)$. If $F'(0) > 0$, then $f^*(u)$ has a unique root located at $u = k^{-1}(M)$.*

Proof. Examine the following properties of the function $f^*(u)$:

$$\lim_{u\to 0^+} f^*(u) = -\infty$$
$$\lim_{u\to 1^-} f^*(u) = 0$$
$$\lim_{u\to 1^-} \frac{df^*(u)}{du} = \frac{m\left[2(m+1)-K\right]}{2(m+1)}.$$

The third limit corresponds exactly with the condition for the initial behaviour of the prey nullcline from (3.3). The derivative of f^* at $u = 1$ is positive when the prey nullcline $F(x)$ is initially decreasing, and negative when $F(x)$ is initially increasing. This implies that $f^*(u)$ must have at least one root for $0 < u < 1$ when the prey nullcline is initially increasing. In fact, by examining the structure of $f^*(u)$ we see that there must be exactly one root of $f^*(u)$ when the nullcline is initially increasing, since $f^* = 0$ corresponds to having $F'(k(u)) = 0$. Thus, the unique zero occurs when $k(u) = M$, i.e. $u = k^{-1}(M)$. To show that no root exists when $F'(0) \leq 0$, it suffices to show that $f^*(u)$ is increasing on $(0, 1)$.

$$\begin{aligned} f^*(u) &= f_1(k(u)) \\ f^{*'}(u) &= k'(u)f_1'(k(u)) \\ &= k'(u)\left[(m + q'(x))F'(x) + (mx + q(x))F''(x))\right]\Big|_{x=k(u)} > 0. \end{aligned}$$

Since $F(x)$ is decreasing and concave down for $0 < x < K$, we have $F''(k(u)) = f'(k(u)) < 0$. Thus, $f^{*'}(u) > 0$ for $0 < u < 1$ implies that f^* is a negative, increasing function with no roots in the interval $0 < u < 1$. □

Corollary 5.9.1. *If $F'(0) \leq 0$, then system (2.8) has no periodic orbits.*

Proof. By condition $(iii)'$ this is equivalent to showing that there exists some $c \in \mathbb{R}$ such that $f^* - cg^*$ has no roots. Take $c = 0$ here. By Lemma 5.9, $f^*(u)$ has no roots in $(0, 1)$, and so condition $(iii)'$ is satisfied. Hence no limit cycle exists. □

Remark. *The result given in Corollary 5.9.1 was already established using the Lyapunov function in (4.6) and the LaSalle Extension Theorem. This merely offers an alternative method to obtain an identical result.*

Lemma 5.10. *Let $x = I$ denote the unique inflection point of $F(x)$, and let $u_I = k^{-1}(I)$ and $u_M = k^{-1}(M)$ represent the u coordinate corresponding to the inflection point and local maximum of $F(x)$, respectively. Then $f^*(u)$ is decreasing for $u_I \leq u < 1$ and $f^*(u)$ is increasing for $0 < u \leq u_M$.*

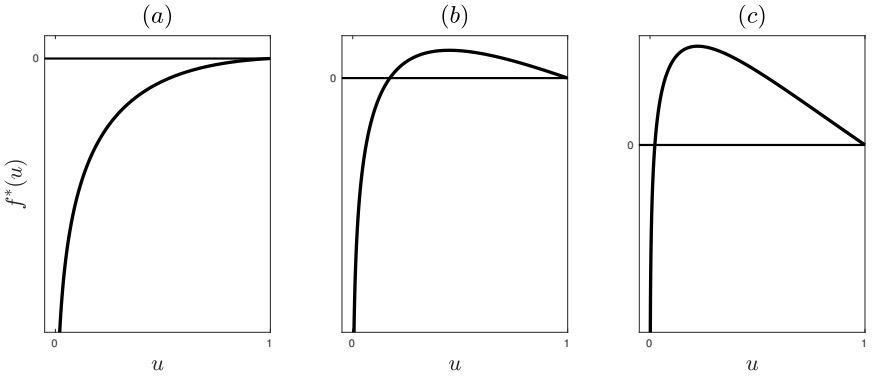

Figure 5.1: *The three possible configurations for $f^*(u)$. The parameter m is fixed at $m = 0.25$ and K is varied from (a) $K = 2$, (b) $K = 6$, (c) $K = 12$. Plot (a) occurs when the prey nullcline is initially flat or decreasing. When the nullcline is initially increasing $f^*(u)$ may take the shape of either (b) or (c), where (b) is strictly concave down and (c) has a unique inflection point to the right of the local maximum.*

Proof. Examine the first derivative of $f^*(u)$:

$$\begin{aligned} f^{*'}(u) &= k'(u) f_1'(k(u)) \\ &= k'(u) \left[(m + q'(x)) F'(x) + (mx + q(x)) F''(x) \right] \Big|_{x=k(u)}. \end{aligned}$$

If $0 < x \leq I$, we have both $F'(x) > 0$ and $F''(x) \geq 0$ so $f^{*'} < 0$ and $f^*(u)$ is decreasing over the corresponding u interval $u_I \leq u < 0$. Similarly, if $M \leq x < K$ both $F'(x) \geq 0$ and $F''(x) > 0$ so $f^{*'} > 0$ and $f^*(u)$ is increasing over the corresponding u interval $0 < u \leq u_M$. □

We conjecture that $f^*(u)$ can have at most one local maximum. This would be the case if the sign of $f^{*'}(u)$ changed sign exactly once in the interval $u_M < u < u_I$. Additionally, we know that since $x^* < M$, the maximum of f^* must lie to the right of its root. We also conjecture that f^* can have at most one inflection point to the right of its local maximum. This gives the three possible configurations for $f^*(u)$ that are shown in Figure 5.1.

Theorem 5.11. *Assume $f^*(u)$ has one of the three configurations shown in Figure 5.1. That is, $f^*(u)$ is continuously differentiable on $(0, 1)$, $\lim_{u \to 0^+} f^*(u) = -\infty$, $\lim_{u \to 1^-} f^*(u) = 0$, and one of the following holds:*

(a) $f^{*'}(u) > 0$ and $f^{*''}(u) < 0$ for $0 < u < 1$ (Figure 5.1 (a)).

(b) $f^*(u)$ has a unique local maximum to the right of its root, and $f^{*''}(u) < 0$

for $0 < u < 1$ (Figure 5.1 (b)).

(c) *$f^*(u)$ has a unique local maximum to the right of its root, and a unique inflection point to the right of that maximum. (Figure 5.1 (c)).*

Then, if (x^*, y^*) is unstable, system (2.8) has a unique hyperbolic limit cycle, and if (x^*, y^*) is locally stable, then it is globally asymptotically stable.

Proof. This proof proceeds in the same way as the proof of Theorem 2.4 from [17], by considering three cases based on the different configurations of $f^*(u)$ as shown in Figure 5.1.

Case (a): We have $F'(0) \leq 0$. Thus $F'(x) < 0$ for $0 < x < K$, so the equilibrium point is always locally stable. By Corollary 5.9.1 no periodic orbits exist, so (x^*, y^*) is globally asymptotically stable. In cases (b) and (c), $F'(0) > 0$, so $F(x)$ has an interior local maximum.

Case (b): Let u_g be the unique root of the linear function $g^*(u)$ and u_f be the unique root of $f^*(u)$ on $0 < u < 1$. Distinguish two sub-cases based on the relative positioning of u_g and u_f. The first case is $u_g \leq u_f$, corresponding to $x^* \geq M$ in the original coordinate system. In this case the coexistence equilibrium point is locally stable, so we seek to prove that no periodic orbits exist. Following Theorem 5.5, choose c to be given by

$$c = \left.\frac{f^{*'}(u)}{g^{*'}(u)}\right|_{u=u_g}. \tag{5.6}$$

Then $c < 0$ and since $g^*(u)$ is linear,

$$\frac{d^2}{du^2}\left[f^*(u) - cg^*(u)\right] = \frac{d^2}{du^2} f^*(u) < 0. \tag{5.7}$$

Since the second derivative is negative, the first derivative of $f^*(u) - cg^*(u)$ has exactly one root at $u = u_g$. Thus, $f^*(u) - cg^*(u)$ obtains an absolute maximum at $u = u_g$, and $f^*(u_g) \leq 0$. Therefore, this choice of c gives $f^*(u) - cg^*(u) < 0 \ \forall \ 0 < u < 1$. By condition $(iii)'$ of Theorem 5.5, no limit cycles exist so the coexistence equilibrium point is globally asymptotically stable. For the second sub-case we have $u_g > u_f$. This corresponds to having $x^* < M$, so the coexistence equilibrium point is unstable. By Lemma 5.6 we only need to show that no repeated roots of $f^*(u) - cg^*(u)$ are possible on $0 < u < u_f$ and $u_g < u < 1$. On both of these intervals $f^*(u)$ and $g^*(u)$ have opposite signs, so $c < 0$ is necessary for a root to exist. However, evaluating at $u = u_g$ and $u = u_f$, $f^* - cg^* > 0$, so in order to have a repeated root the function would need to be concave up. By (5.7) this is not the case, so it follows that

$f^*(u) - cg^*(u)$ cannot have multiple zeros on $0 < u < 1$. Thus, condition $(iii)''$ is satisfied and there is a unique, hyperbolic limit cycle.

Case (c): Let u_i be the unique inflection point of $f^*(u)$. Again there are two cases to consider based on the positions of u_g and u_f. First, for $u_g \leq u_f$ take c as in (5.6). On the interval $0 < u < u_i$ the same proof as for the previous cases holds. Next, on the interval $u_i < u < 1$ we have $f^{*''}(u) > 0$. Also, on this interval $f^{*'}(u) < 0$, $g^{*'}(u) < 0$ and $c < 0$, so $f^*(u) - cg^*(u)$ is monotonically decreasing on $u_i < u < 1$. Since $f^*(u) - cg^*(u) < 0$ on $0 < u < u_i$ and is decreasing on $u_i < u < 1$, it follows that $f^*(u) - cg^*(u) < 0$ for $0 < u < 1$. Thus, condition $(iii)'$ holds and no limit cycles exist on $u_i < u < 1$. The second sub-case is again $u_g > u_f$. On $0 < u < u_i$ the proof from the previous cases holds. On the interval $u_i < u < 1$ it is necessary to again subdivide into two cases based on the relative positions of u_i and u_g. First consider $u_g \leq u_i$. On the interval $u_i < u < 1$ note that the derivatives of f^* and g^* have the same signs but the first derivatives of f^* and g^* have opposite signs. Thus, it is impossible for $f^*(u) - cg^*(u)$ to have a double root for any choice of $c \in \mathbb{R}$. Finally, consider $u_g > u_i$. An application of Lemma 5.6 allows us to only consider the interval $u_g < u < 1$. Again in this case, f^* and g^* have opposite signs, but their derivatives have the same sign. Thus it is not possible for $f^*(u) - cg^*(u)$ to have a double root for any choice of c. Therefore, for $u_g > u_f$, by condition $(iii)''$, system (2.8) has a unique hyperbolic limit cycle. □

In practice, this theorem can be applied by first creating a plot of $f^*(u)$ and examining its properties for the desired parameters. If the shape is one of the three displayed in Figure 5.1, then by Theorem 5.11, if (x^*, y^*) is locally stable, then it is globally asymptotically stable, and if (x^*, y^*) is unstable, then it is surrounded by a unique, stable periodic orbit.

Chapter 6

Bifurcation Analysis

This chapter investigates changes in the dynamics of system (2.8) as the parameters are varied. The primary focus will be to vary S^0, with D used as a secondary bifurcation parameter.

First, if $S^0m - D < 0$, then the zero equilibrium $E_0 = (0, 0)$ is the only equilibrium point that exists and it is globally asymptotically stable. As S^0 is increased to the point where $S^0m - D > 0$, solutions become biologically interesting and the $E_1 = (K, 0)$ equilibrium becomes globally stable. Further increasing S^0 gives rise to a second transcritical bifurcation at $x^* = M$, when the E_1 and $E_* = (x^*, y^*)$ equilibria exchange stability. Finally, we know from (4.4) that the coexistence equilibrium loses its stability for $x^* < M$.

Proposition 6.1. *System (2.8) has a Hopf bifurcation occurring at* $(x^*, y^*) = (M, F(M))$.

Proof. Recall from Proposition 5.2 that if a periodic orbit exists in this system, then it must surround the coexistence equilibrium E_*. This makes E_* the only possibility for a Hopf bifurcation to occur in this system. The eigenvalues of the Jacobian matrix (4.4) evaluated at E_* are

$$\lambda_{+,-} = \frac{1}{2}\left(-(mx^* + D)F'(x^*)\right) \pm \frac{1}{2}\sqrt{\left((mx^* + D)F'(x^*)\right)^2 - 4y^*q'(x^*)(mx^* + D)}. \quad (6.1)$$

When the coexistence equilibrium exists, these eigenvalues are purely imaginary if and only if $F'(x^*) = 0$. The condition $F'(x^*) = 0$ can be achieved

by fixing $K = \hat{K}$ from (3.14). Also, the imaginary part of the eigenvalues is non-zero. Furthermore, the transversality condition holds, since the derivative with respect to K of the real part of the eigenvalue at the Hopf bifurcation is positive by (3.13). Thus, the eigenvalues are complex in a neighbourhood of $\hat{K}$ and cross the imaginary axis at $K = \hat{K}$, implying that a Hopf bifurcation occurs there. □

6.1 Vague Attractor Condition

Conditions were determined by Andronov [1] and Hopf [12] for a phenomenon that has become known as the Andronov-Hopf bifurcation. They proved that if the real part of the eigenvalues at an equilibrium considered as a function of a single parameter cross the imaginary axis transversally, then a family of periodic orbits is born. In Marsden and McCracken [23] a formula is derived to determine for which values of the parameter the bifurcating periodic orbits exist, and also to determine their stability. The formula is based on determining the stability of the equilibrium point at the Hopf bifurcation using higher order terms. In order to use their formula, we need to evaluate the Jacobian of system (2.8) at the equilibrium, assuming it is a function of the bifurcation parameter. We then make a change of variables to put this Jacobian into real Jordan Canonical Form (RJCF), J:

$$\begin{pmatrix} u \\ v \end{pmatrix}' = J \begin{pmatrix} u \\ v \end{pmatrix} + H.O.T. = \begin{pmatrix} f(u,v) \\ g(u,v) \end{pmatrix}.$$

For a system in this form, Marsden and McCracken derived the following formula for the so-called vague attractor condition:

$$\begin{aligned} V''' = &\frac{3\pi}{4|\beta|}(f_{uuu} + f_{uvv} + g_{uuv} + g_{vvv}) \\ &+ \frac{3\pi}{4|\beta|^2}(-f_{uv}(f_{uu} + f_{vv}) + g_{uv}(g_{uu} + g_{vv}) + f_{uu}g_{uu} - f_{vv}g_{vv}). \end{aligned} \quad (6.2)$$

If $V''' < 0$, then the equilibrium is a vague attractor and the family of bifurcating periodic orbits are all orbitally asymptotically stable.

The evaluation of expressions in this section was done using the computational software Maple [22]. First, the Jacobian matrix $A \triangleq J|_{(x^*,y^*)}$ in (4.4) must be transformed into RJCF. That is, we must find an invertible matrix P

such that:

$$J = P^{-1}AP = \begin{pmatrix} \alpha & \beta \\ -\beta & \alpha \end{pmatrix}, \tag{6.3}$$

where the eigenvalues of A are $\lambda_{+,-} = \alpha \pm i\beta$.

Lemma 6.2. *The invertible matrix P needed to transform A into RJCF is given by $P = (P_{re} \;\; P_{im})$, where P_{re} and P_{im} are the real and imaginary parts, respectively, of the eigenvector v_+ associated with eigenvalue λ_+.*

Proof.

$$\begin{aligned} \begin{pmatrix} 1 & 0 \\ 0 & 1 \end{pmatrix} &= P^{-1}P \\ &= P^{-1}\begin{pmatrix} P_{re} & P_{im} \end{pmatrix} \\ &= \begin{pmatrix} P^{-1}P_{re} & P^{-1}P_{im} \end{pmatrix}. \end{aligned}$$

Thus, $P^{-1}P_{re} = \begin{pmatrix} 1 \\ 0 \end{pmatrix}$ and $P^{-1}P_{im} = \begin{pmatrix} 0 \\ 1 \end{pmatrix}$. Now examine the eigenvalue equation.

$$\begin{aligned} Av_+ &= \lambda_+ v_+ \\ A(P_{re} + iP_{im}) &= (\alpha + i\beta)(P_{re} + iPim). \end{aligned}$$

Setting the real and imaginary parts of this equation equal gives

$$\begin{aligned} AP_{re} &= \alpha P_{re} - \beta P_{im} \\ AP_{im} &= \beta P_{re} + \alpha P_{im}. \end{aligned}$$

Finally, substituting into the equation for J, we get

$$\begin{aligned} J &= P^{-1}AP \\ &= P^{-1}\begin{pmatrix} AP_{re} & AP_{im} \end{pmatrix} \\ &= P^{-1}\begin{pmatrix} \alpha P_{re} - \beta P_{im} & \beta P_{re} + \alpha P_{im} \end{pmatrix} \\ &= \begin{pmatrix} \alpha P^{-1}P_{re} - \beta P^{-1}P_{im} & \beta P^{-1}P_{re} + \alpha P^{-1}P_{im} \end{pmatrix} \\ &= \begin{pmatrix} \alpha \begin{pmatrix} 1 \\ 0 \end{pmatrix} - \beta \begin{pmatrix} 0 \\ 1 \end{pmatrix} & \beta \begin{pmatrix} 1 \\ 0 \end{pmatrix} + \alpha \begin{pmatrix} 0 \\ 1 \end{pmatrix} \end{pmatrix} \\ &= \begin{pmatrix} \alpha & \beta \\ -\beta & \alpha \end{pmatrix}. \end{aligned} \tag{6.4}$$

Therefore, $P = \begin{pmatrix} P_{re} & P_{im} \end{pmatrix}$ is the invertible matrix P needed to convert J into RJCF. □

To convert the Jacobian matrix from (4.4) into RJCF, first examine its eigenvalues in (6.1). Thus, take α and β to be

$$\alpha = \frac{1}{2}(mx^* + D)F'(x^*)$$
$$\beta = \frac{1}{2}\sqrt{-((mx^* + D)F'(x^*))^2 + 4q'(x^*)y^*(mx^* + D)}.$$

The matrix P can be constructed by considering the real and imaginary parts of the eigenvector corresponding to λ_+

$$P = \begin{pmatrix} \frac{(mx^*+D)F'(x^*)}{2y^*q'(x^*)} & \frac{\sqrt{(mx^*+D)(-F'(x^*)^2(mx^*+D)+4y^*q'(x^*))}}{2y^*q'(x^*)} \\ 1 & 0 \end{pmatrix} \tag{6.5}$$

Using this P, we can finally rewrite our system so that its linear part is in RJCF,

$$\begin{aligned} \begin{pmatrix} x \\ y \end{pmatrix}' &= A \begin{pmatrix} x \\ y \end{pmatrix} + H.O.T. \\ P^{-1} \begin{pmatrix} x \\ y \end{pmatrix}' &= P^{-1}A \begin{pmatrix} x \\ y \end{pmatrix} + P^{-1}(H.O.T.) \\ &= P^{-1}APP^{-1} \begin{pmatrix} x \\ y \end{pmatrix} + P^{-1}(H.O.T.) \\ &= JP^{-1} \begin{pmatrix} x \\ y \end{pmatrix} + P^{-1}(H.O.T.). \end{aligned} \tag{6.6}$$

Now, performing the change of variables $\begin{pmatrix} u \\ v \end{pmatrix} = P^{-1} \begin{pmatrix} x \\ y \end{pmatrix}$, system (2.8) becomes

$$\begin{pmatrix} u \\ v \end{pmatrix}' = J \begin{pmatrix} u \\ v \end{pmatrix} + H.O.T. = \begin{pmatrix} f(u,v) \\ g(u,v) \end{pmatrix}. \tag{6.7}$$

In the chemostat system,

$$P^{-1} \begin{pmatrix} x' \\ y' \end{pmatrix} = \begin{pmatrix} y(q(x) - D) \\ \frac{2y^*q'(x^*)(q(x)+mx)(F(x)-y)-F'(x^*)(mx^*+D)y(q(x)-D)}{\sqrt{(mx^*+D)(-F'(x^*)^2mx^*-F'(x^*)^2D+4y^*q'(x^*))}} \end{pmatrix} = \begin{pmatrix} f(x,y) \\ g(x,y) \end{pmatrix}$$

Consider $x = x(u,v)$ and $y = y(u,v)$. Then the change of variables can be inverted to find x and y in terms of u and v.

$$\begin{pmatrix} x \\ y \end{pmatrix} = P \begin{pmatrix} u \\ v \end{pmatrix} = \begin{pmatrix} \frac{F'(x^*)(mx^*+D)u+\sqrt{(mx^*+D)(-F'(x^*)^2mx^*-F'(x^*)^2D+4y^*q'(x^*))v}}{2y^*q'(x^*)} \\ u \end{pmatrix}.$$

We can now use the chain rule to compute the vague attractor condition from (6.2) for the chemostat

$$V'''(x^*, y^*, \hat{K}) = \frac{(mx^* + D)(2F''(x^*)q'(x^*)(q'(x^*) + m) + F'''(x^*)q'(x^*)D)}{y^*q'(x^*)^2} - \frac{(mx^* + D)(q''(x^*)F''(x^*)(mx^* + D) - F'''(x^*)q'(x^*)mx^*)}{y^*q'(x^*)^2}.$$

The sign of V''' is what we wish to determine, so factoring out the positive constant $\frac{mx^*+D}{y^*q'(x^*)^2}$, we have $sgn(V''') = sgn(w)$, where

$$w = (mx^* + D)(F'''(x^*)) - \frac{(mx^* + D)F''(x^*)q''(x^*)}{q'(x^*)} + 2(q'(x^*) + m)F''(x^*).$$

Substituting the Ivlev functional response along with the Hopf bifurcation condition $K = \hat{K}$, the criticality condition w becomes

$$w = \frac{m[(D-1)(D+m-1)\ln(1-D)^2 + (-4D^2 + 6D - 2m - 2)\ln(1-D)}{(-m\ln(1-D) + D)((D-1)\ln(1-D) - D)} + \frac{4D^2 - 2D(m+1)]}{(-m\ln(1-D) + D)((D-1)\ln(1-D) - D)}. \quad (6.8)$$

6.2 Criticality of the Hopf Bifurcation

The criticality of the Hopf bifurcation is then determined by the sign of w. If $w < 0$, the Hopf bifurcation is supercritical and if $w > 0$, then it is subcritical.

Proposition 6.3. *The Hopf bifurcation in system (2.8) at $x^* = M$ is always supercritical.*

Proof. To determine the sign of w, first consider the denominator. Clearly $(-m\ln(1-D)+D) > 0$ since $0 < D < 1$. Recall $\nu(D) = (D-1)\ln(1-D) - D < 0$ for $0 < D < 1$ from (4.14). Thus the denominator of w is negative.

For the numerator, since $m > 0$, we first divide through by m. Denote the remaining part of the numerator by ξ and notice that it is linear in m. As such, consider ξ as a function of m.

$$\xi(m) \triangleq [(D-1)\ln^2(1-D) - 2\ln(1-D) - 2D]m + (D-1)^2\ln(1-D)^2 + (-4D^2 + 6D - 2)\ln(1-D) + 4D^2 - 2D.$$

First determine the sign of ξ at $m = 0$.

$$\begin{aligned}\xi(0) &= (D-1)^2\ln^2(1-D) + (-4D^2+6D-2)\ln(1-D) + 4D^2 - 2D \\ &= (D-1)^2\ln^2(1-D)^2 - 2(2D-1)\nu(D),\end{aligned}$$

where $\nu(D) < 0$ as before. Now consider $\xi(0)$ as D is varied in $(0,1)$.

$$\begin{aligned}\xi(0)\Big|_{D=0} &= 0 \\ \frac{d}{dD}\xi(0) &= 2\nu(D)\left(\ln(1-D) - 2\right) > 0 \quad \forall\ 0 < D < 1.\end{aligned}$$

Thus $\xi(0) > 0$ for $0 < D < 1$. Now examine $\xi'(m)$:

$$\begin{aligned}\xi'(m) &= (D-1)\ln^2(1-D) - 2\ln(1-D) - 2D \\ \xi'(m)\Big|_{D=0} &= 0 \\ \frac{d}{dD}\xi'(m) &= \ln^2(1-D) + 2\left(\frac{D}{1-D} + \ln(1-D)\right).\end{aligned}$$

Let $\psi(D) = \frac{D}{1-D} + \ln(1-D)$. Then $\psi(0) = 0$ and $\psi'(D) = \frac{D}{(1-D)^2} > 0$, so $\psi(D) > 0$ for $0 < D < 1$. As such, $\frac{d}{dD}\xi'(m) > 0$ so $\xi'(m) > 0$ for $0 < D < 1$. Since $\xi(0) > 0$ and $\xi'(m) > 0$, it can be concluded that $\xi(m) > 0\ \forall\ m > 0$ and $0 < D < 1$. Therefore, $w < 0$ so the Hopf bifurcation which occurs at $x^* = M$ is always supercritical. □

6.3 Bifurcation Results

The bifurcation results are summarized in Figure 6.1 (generated using XPPAUT [7] and plotted using Matlab [24]). The two transcritical bifurcations are seen along with the supercritical Hopf. The first transcritical bifurcation occurs when $S^0 m - D = 0$ and solutions become biologically relevant. Stability passes from E_0 to E_1 when this occurs. The second transcritical bifurcation occurs at $x^* = K$, and stability is passed from E_1 to E_*. Finally, the supercritical Hopf bifurcation at $x^* = M$ shows a transfer of stability from E_* to a periodic orbit.

We can also consider a two parameter bifurcation diagram for system (2.8) with Ivlev functional response by taking D as the secondary bifurcation parameter. This is illustrated in Figure 6.2. The two parameter bifurcation

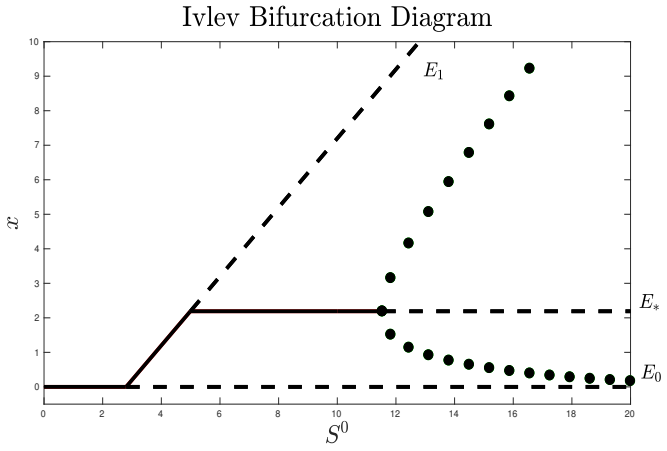

Figure 6.1: *The bifurcation diagram for the system with Ivlev functional response and S^0 as the primary bifurcation parameter. The other parameters are fixed at $m = 0.25$, $D = 0.7$, $a = 0.87565$ and $b = 0.73332$. Solid lines correspond to stable equilibria, dashed lines correspond to unstable equilibria and filled circles correspond to the largest and smallest values of x on a stable periodic orbit. E_0 represents the $(0, 0)$ equilibrium, E_1 is the $(K, 0)$ equilibrium and E_* is the (x^*, y^*) equilibrium.*

diagram separates the (S^0, D) plane into regions with different dynamics. In R_1 solutions converge asymptotically to the only equilibrium point, E_0. In R_2 two equilibria exist, E_0 and E_1. Solutions with positive initial conditions converge to the E_1 equilibrium. In R_3 all three equilibrium points exist, and there is global asymptotic convergence to the coexistence equilibrium E_* for positive initial conditions. Finally, R_4 again has all of the equilibrium points existing, but solutions converge to a stable periodic orbit surrounding E_*.

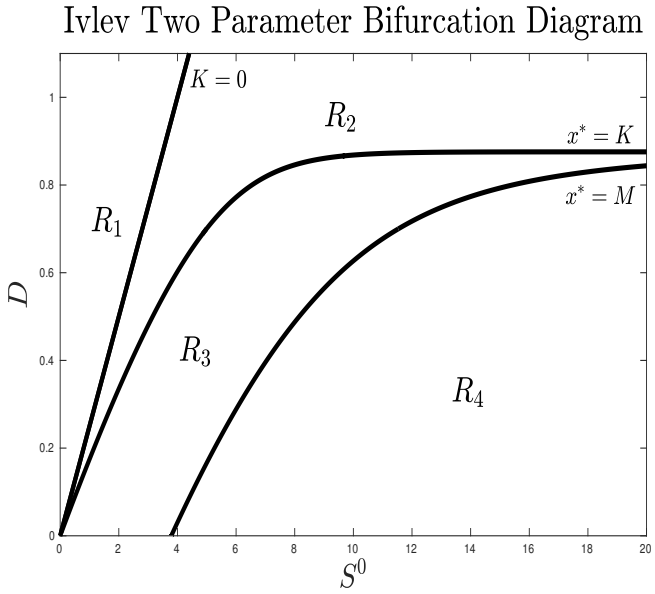

Figure 6.2: *The two parameter bifurcation diagram for the chemostat with Ivlev functional response.* S^0 *is used as the primary and* D *the secondary bifurcation parameters. The other parameters are fixed at* $m = 0.25$, $a = 0.87565$ *and* $b = 0.73332$. *The line separating* R_1 *and* R_2 *is the transcritical bifurcation between* E_0 *and* E_1 *that occurs when* $K = 0$. *The curve between* R_2 *and* R_3 *is the transcritical bifurcation when* E_1 *exchanges stability with* E_* *at* $x^* = K$. *The curve separating* R_3 *and* R_4 *is the Hopf bifurcation of* E_* *that occurs when* $x^* = M$.

Chapter 7

Extension to the 3D System

With the analysis of the 2D system complete, it remains to justify that the dynamics of subsystem (2.8) are equivalent to those of the 3D system from (2.4). The existence and uniqueness of solutions follows directly from that of the 2D system, as does the existence and number of periodic orbits. Additionally, there is a direct correspondence between the equilibrium points of the 2D and 3D systems, since it was previously shown that solutions of (2.4) converge to the 2D simplex $S+x+y = S^0$. Thus, the three equilibrium points of the 3D system are $E_0 = (S^0, 0, 0)$, $E_1 = (S^0 - K, K, 0)$ and $E_* = (S^0 - x^* - y^*, x^*, y^*)$. The local stability of these equilibria from Chapter 4 remains unchanged, since the additional eigenvalue must be negative in order for the solution to converge to the simplex.

To prove that when an equilibrium is globally asymptotically stable for the 2D system (2.8), then the corresponding equilibrium of the 3D system is globally asymptotically stable in (2.4), we use the Butler McGehee Lemma as stated by Freedman and Waltman [2]. Let $\mathcal{O}(X)$ denote the orbit through a point X, and $\omega(X)$ denote the omega limit set of $\mathcal{O}(X)$. Also, if P is a hyperbolic equilibrium point, then let $M^+(P)$ and $M^-(P)$ denote its stable and unstable manifolds, respectively.

Lemma 7.1. *(Butler McGehee Lemma) Let P be an isolated hyperbolic equilibrium point in the omega limit set $\omega(X)$ of an orbit $\mathcal{O}(X)$. Then either $\omega(X) = P$ or there exist points Q^+ and Q^- in $\omega(X)$ with $Q^+ \in M^+(P)$ and $Q^- \in M^-(P)$.*

For the chemostat model (2.4), take $X = (S, x, y)$ with $S \geq 0$, $x \geq 0$, and $y \geq 0$. Let $\mathcal{O}(X)$ be the orbit through point X, and $\omega(X)$ be the omega

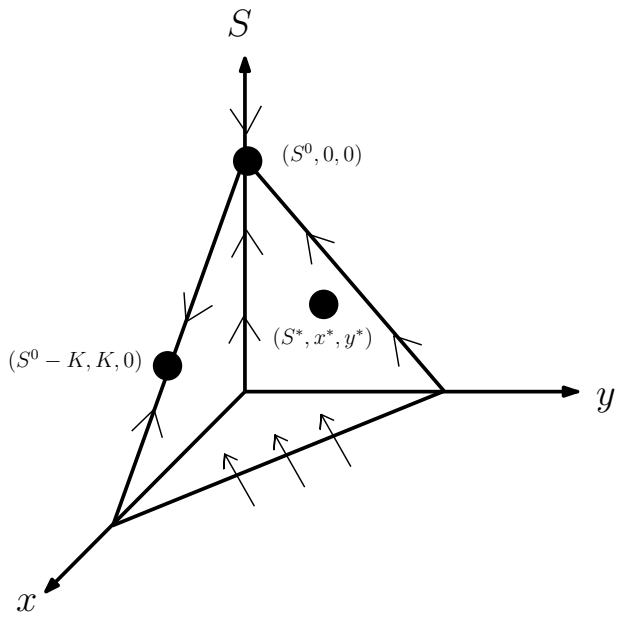

Figure 7.1: *The dynamics on the boundary of the $S + x + y = S^0$ simplex when all three equilibium points exist.*

limit set of $\mathcal{O}(X)$. Note that by Lemma 2.1, $\omega(X)$ is bounded. Let $E_0 = (S^0, 0, 0)$ represent the equilibrium corresponding to extinction of both species, $E_1 = (S^0 - K, K, 0)$ correspond to predator extinction and E_* correspond to the coexistence equilibrium. Also, let $\mathcal{S} = \{(S, x, y) : S \geq 0, x \geq 0, y \geq 0, S + x + y = S^0\}$.

Proposition 7.2. *When $K \leq 0$, then $(0, 0)$ is globally asymptotically stable for the 2D system (2.8) with respect to solutions originating in the first quadrant, and E_0 is globally asymptotically stable in the 3D system (2.4), with respect to solutions originating in the first octant.*

Proof. When $K \leq 0$, $(0, 0)$ is the only equilibrium point of (2.8). Consider a point $X \in \mathbb{R}^3_+$. If X lies on $\mathcal{S}$, then $E_0 \in \omega(X)$ since E_0 is globally stable for the 2D system. If X does not lie on $\mathcal{S}$, then by (2.5), there is a point in $\omega(X)$ which lies on $\mathcal{S}$. This implies $E_0 \in \omega(X)$. Since E_0 is asymptotically stable, it is the only point in $\omega(X)$. Therefore, when E_0 is the only equilibrium point, it is globally asymptotically stable for system (2.4) with non-negative initial conditions. □

Proposition 7.3. *The equilibrium point $(K, 0)$ is globally asymptotically stable for system (2.8) when $K > 0$, $q^{-1}(D) > K$, $x(0) > 0$, and $y(0) \geq 0$. If in*

addition, $S(0) \geq 0$, then E_1 is globally asymptotically stable for the 3D system (2.4), with respect to initial conditions $S(0) \geq 0$, $x(0) > 0$, and $y(0) \geq 0$.

Proof. In this case, $K > 0$, and the only equilibrium points which lie on the simplex $\mathcal{S}$. On $\mathcal{S}$, all orbits with $x(0) > 0$ will converge to E_1. Now take X in the interior of $\mathbb{R}^3_+$, and suppose $E_0 \in \omega(X)$. Since E_0 is a saddle point, it cannot be the only point in $\omega(X)$. The stable manifold $M^+(E_0)$ is the two dimensional $S - y$ plane, that by the Bulter McGehee Lemma, must also contain a point $Q^+ \neq E_0$ in $\omega(X) \cap M^+(E_0)$. However, if $Q^+ \in \omega(X)$, then the entire orbit through Q^+ is also in $\omega(X)$, contradicting the boundedness of $\omega(X)$. Therefore, $E_0 \notin \omega(X)$ for X in the interior of $\mathbb{R}^3_+$. Next, suppose there is a point in the ω-limit set of X that lies on the $S - y$ plane. Then we would have $E_0 \in \omega(X)$, which is a contradiction. Thus, for all choices of X with $x > 0$, $E_1 \in \omega(X)$. We therefore have global asymptotic stability of E_1 in system (2.4) whenever $K > 0$, $x^* > K$, and $x(0) \neq 0$. □

A visualization of the dynamics on the boundary of the simplex when all three equilibrium points exist is given in Figure 7.1. By applying the Butler McGehee lemma, all trajectories with positive initial conditions converge to the interior of the $S + x + y = S^0$ simplex and obey the dynamics of the 2D subsystem on that simplex. When (x^*, y^*) is globally asymptotically stable in the 2D subsystem (2.8), we will prove that the coexistence equilibrium E_* is globally asymptotically stable in the original 3D model.

Proposition 7.4. *When (x^*, y^*) is globally asymptotically stable for the 2D system (2.8) with respect to initial conditions $x(0) > 0$, and $y(0) > 0$, then E_* is globally asymptotically stable in the 3D system (2.4), with respect to initial conditions $S(0) \geq 0$, $x(0) > 0$, and $y(0) > 0$.*

Proof. In the case where E_* exists, all three equilibrium points of system (2.4) lie on $\mathcal{S}$. Since (x^*, y^*) is globally asymptotically stable in the 2D system there are no periodic orbits on $\mathcal{S}$. Note by (2.5) that $\omega(X)$ is contained in $\mathcal{S}$. We must show that for X in the interior of $\mathbb{R}^3_+$, E_* is the only point in $\omega(X)$.

First suppose that $E_0 \in \omega(X)$. Since E_0 is a saddle point, it cannot be the only point in $\omega(X)$, so by Lemma 7.1 there must be at least one other point $Q^+ \in \omega(X) \cap M^+(E_0)$. The two dimensional stable manifold of E_0 is the positive $S - y$ plane, which contains the S axis. Since the entire orbit through Q^+ is contained in $\omega(X)$, the entire positive S axis must be in $\omega(X)$, contradicting its boundedness. Thus, E_0 cannot be in the omega limit set of $\mathcal{O}(X)$ for X in the interior of the positive octant. We also show that

$E_1 \notin \omega(X)$, since if E_* exists, then E_1 is a saddle point. Again by Lemma 7.1 there must exist a point $Q^- \in \omega(X) \cap M^-(E_1)$. The one dimensional unstable manifold of E_1 is the positive y direction, which implies $E_* \in \omega(X) \cap M^-(E_1)$. Since E_* is asymptotically stable with respect to the 3D system, E_* must be the only point in $\omega(X)$. Thus $E_1 \notin \omega(X)$.

Next, assume that $\omega(X)$ contains a point that lies on the $S - y$ plane. This implies $E_0 \in \omega(X)$, a contradiction. Finally, assume that $\omega(X)$ contains a point that lies on the $S - x$ plane. Then, either $E_1 \in \omega(X)$, or $\omega(X)$ is unbounded, both contradictions. Therefore, $\omega(X) = \{E_*\}$ for X in the interior of $\mathbb{R}^3_+$. □

Chapter 8

Comparison with Monod Response

The focus of this chapter is to explore the sensitivity of the model to the functional form chosen for $q(x)$. As previously discussed, the Ivlev and Monod forms both have the necessary requirements for the predator response function, and by looking at the theoretical sample data alone it is statistically impossible to determine which, if either, form should be chosen.

8.1 Monod Preliminary Analysis

First, some preliminary analysis on the prey isocline with Monod form is required. The initial behaviour of the prey nullcline is determined by the signs of $F'(0)$ and $F''(0)$. For the Monod response,

$$\begin{aligned} F_{M}'(0) &\triangleq \lim_{x\to 0} {F_{M}}'(x) = \frac{m\left(K-(m+1)\right)}{(m+1)^2} \\ &\leq 0 \text{ if } K \leq m+1 \\ &> 0 \text{ if } K > m+1 \end{aligned} \tag{8.1}$$

$$F_{M}''(x) = \frac{-2m\left(Km+m+1\right)}{(mx+m+1)^3} \tag{8.2}$$

Thus, the prey nullcline for the Monod response can be initially increasing, decreasing or zero, and is concave down for all $x \geq 0$. The prey nullcline

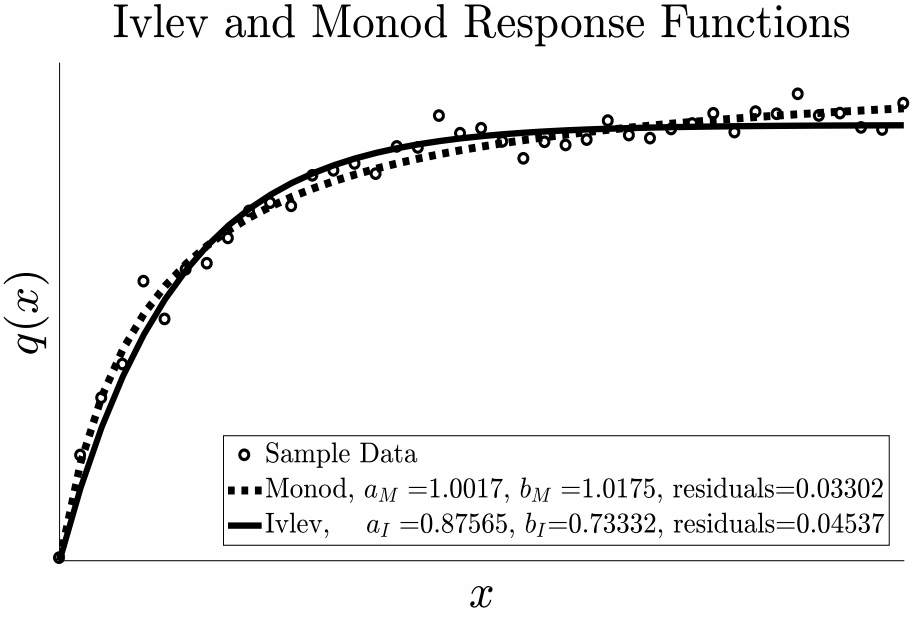

Figure 8.1: *Plots of the Monod and Ivlev response functions with their best fit parameters. The sample data points are only demonstrative and were generated by perturbing the Monod response with* $a = b = 1$. *A non-linear least squares algorithm was then used to generate the parameters* a_M, b_M, a_I *and* b_I. *The sum of the residuals squared is also displayed.*

with Monod response also has at most one extremum, a local maximum. In the Monod case, it is possible to solve for the x value of the local maximum explicitly,

$$M = \frac{-(m+1) + \sqrt{Km + m + 1}}{m}. \tag{8.3}$$

We also have

$$q(x) - xq'(x) = \frac{x^2}{(1+x)^2} > 0.$$

Therefore, by 3.13 the local maximum moves up and to the right as K increases. The local stability of the equilibrium points results from Chapter 4 were done in general and as such are applicable to the Monod form as well as the Ivlev.

8.2 Monod Global Stability and Periodic Orbits

Theorem 8.1. *System (2.8) with Monod functional response has a unique, stable periodic orbit when $x^* < M$.*

Proof. Recall Theorem 5.3, originally by Huang [14]. For the purposes of simplifying this proof, a different scaling of system (2.8) with the Monod response is used. It is more convenient here to scale out the parameter m and instead leave a. This leaves the chemostat model with Monod functional response as

$$\begin{aligned} \frac{dx}{dt} &= (x + q(x))(F(x) - y) \\ \frac{dy}{dt} &= y(-D + q(x)). \end{aligned} \tag{8.4}$$

with $F(x) = \frac{x(K-x)}{x+q(x)}$ and $q(x) = \frac{ax}{1+x}$. The condition under which the coexistence equilibrium exists in this scaling is $0 < D < a$. Take $\phi(x) = x + q(x)$, $\pi(y) = y$, $\rho(y) = y$ and $\psi(x) = -D + q(x)$. This chemostat model now has the same form as Huang's system (5.1). Conditions *(i)*, *(ii)* and *(iii)* are easily verified. It remains to show condition *(iv)* holds, that is $H(x)$ is non-decreasing.

$$\begin{aligned} H'(x) &= \frac{-1}{\psi^2(x)} \left((F''(x)\phi(x) + F'(x)\phi'(x))\psi(x) - F'(x)\phi(x)\psi'(x) \right) \\ &= \frac{h(x)}{(1+x+a)^2((a-D)x - D)^2}, \end{aligned}$$

where $h(x)$ is a polynomial of degree four with the form

$$\begin{aligned} h(x) &= c_4x^4 + c_3x^3 + c_2x^2 + c_1x + c_0 \\ c_4 &= a - D \\ c_3 &= 2a(a-D) + 2(a-2D) \\ c_2 &= Ka(a-D) + 2a^3 - 2a^2D + 3a^2 - 8aD + a - 6D \\ c_1 &= -4D(a+1)^2 \\ c_0 &= D(a+1)(a(K-1)-1). \end{aligned}$$

Clearly the denominator of $H'(x)$ is positive, so the sign of $H'(x)$ depends only on the sign of $h(x)$. Additionally, for a periodic orbit to be present, $F(x)$ must be increasing initially, which implies

$$F'(0) \triangleq \lim_{x\to 0} F(x) = \frac{a(K-1)-1}{(a+1)^2} > 0 \implies a(K-1)-1 > 0. \tag{8.5}$$

This gives $h(0) = c_0 > 0$. It has also been established that for periodic orbits to exist, $x^* < M$. Since $F'(x;K)$ is linear in K, it is possible to solve for $\hat{K}$ such that $F'(x;\hat{K}) = 0$. For the Monod response this value of $\hat{K}$ is given by

$$\hat{K} = \frac{1}{a}\left(x^2 + (2x+1)(a+1)\right). \tag{8.6}$$

Also, recall that as K increases the local maximum moves up and to the right, so to maintain $x^* < M$ we must have $K > \hat{K}$. Next, note that $h(x)$ is an increasing function of K.

$$\frac{\partial}{\partial K}h(x;K) = a(a-D)x^2 + aD(a+1) > 0, \tag{8.7}$$

so $h(x;K) > h(x;\hat{K})\ \forall\ K > \hat{K}$. Evaluating $h(x)$ at $K = \hat{K}$ gives

$$h(x;\hat{K}) = (x-x^*)^2k(x), \tag{8.8}$$

with $k(x) = x^2 + 2\,(a+1)\,x + (a+1)\left(2\,a + 1 + \frac{a}{a-D}\right)$. Thus, $h(x;\hat{K})$ has a double root at $x = x^*$. The discriminant of the quadratic $k(x)$ is $-a(a+1)(a-D+1)(a-D) < 0$ so $k(x)$ has no real roots. Then, either $k(x) < 0$ or $k(x) > 0\ \forall x$. But $h(0) = c_0 > 0 \implies k(0) > 0$ so we have $k(x) > 0\ \forall\ x$. Therefore,

$$0 < (x-x^*)^2k(x) = h(x;\hat{K}) < h(x;K)\ \ \forall\ K > \hat{K} \text{ and } x \neq x^*. \tag{8.9}$$

Thus we have $h(x) > 0\ \forall\ x$ when $0 < x^* < M$, that implies $H'(x) > 0\ \forall\ x \neq x^*$. Therefore, $H(x)$ is non-decreasing as required, so the periodic orbit is stable and unique. □

Corollary 8.1.1. *Consider system (2.8) with Monod functional response. If $x^* \geq M$, then the coexistence equilibrium (x^*, y^*) is globally asymptotically stable.*

Proof. Refer to Theorem 4.2 and notice that the function $\beta(x)$ to which it refers is identical to the function $H(x)$ used to establish uniqueness of the periodic orbit above. Then $\hat{\beta} = h(x; \hat{K}) > 0$, so the conditions of Theorem 4.2 are satisfied and (x^*, y^*) is globally asymptotically stable whenever it is locally stable. □

8.3 Sensitivity to Functional Form

The sensitivity of the classical predator prey model has been well studied (see for example [9, 28]). In this section we examine if this phenomenon transfers over to the chemostat as well. Refer to Figure 8.1, where it can be seen that both the Monod and Ivlev response functions have the same shape and can be fit to theoretical data very well. In practical situations it is likely not known which, if either, of these functions is the correct choice. Yet depending on which function is chosen the dynamics of the chemostat model can change.

Figure 8.2 shows the variations in the values at which bifurcations of the system occur based on which functional response is used. We notice a small difference in where the transcritical bifurcation between $(0, K)$ and (x^*, y^*) occurs, and a very large difference in where the Hopf bifurcation of (x^*, y^*) occurs. From these variations we select parameters where the systems with Monod and Ivlev functional responses have dynamically different solutions. Figure 8.4 displays an example where the Monod response causes predator extinction and convergence to the $(0, K)$ equilibrium, but the Ivlev response yields persistence of both predator and prey populations. Figure 8.5 demonstrates another such example where the Monod response gives a stable periodic orbit, but the system with Ivlev response has global convergence to the coexistence equilibrium. Based on the bifurcation diagrams in Figure 8.2, it can also be seen that the amplitude of the periodic orbit with the Monod response is larger than the amplitude for the Ivlev response when S^0 is large.

To notice an even larger difference in the parameter sets that yield different dynamics, we can overlay the two parameter bifurcation diagrams for the Monod and Ivlev functional responses. This is done in Figure 8.3.

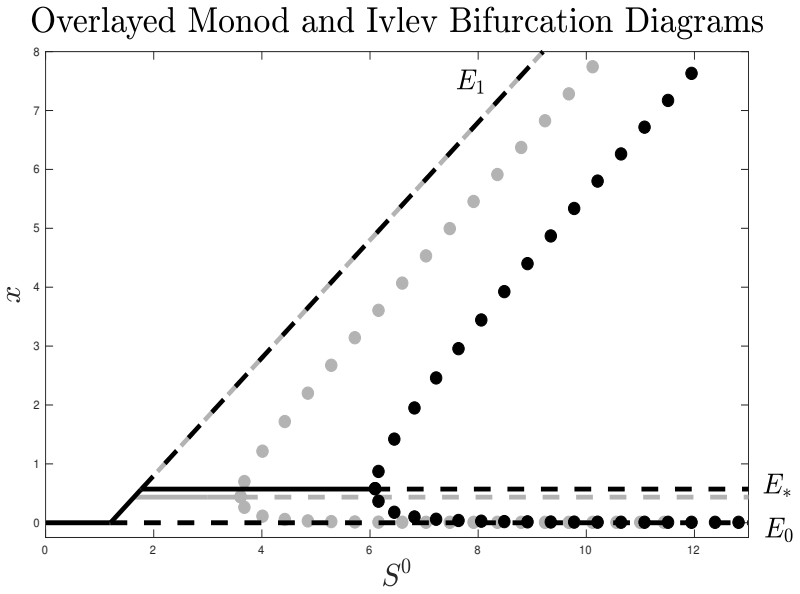

Figure 8.2: *Bifurcation diagrams for the Ivlev and Monod functional forms overlayed. The full opacity plot is Ivlev and the faded plot is Monod. The other parameters are set to* $m = 0.25$, $D = 0.3$, *and* a *and* b *with the best fit values from Figure 8.1. Solid lines correspond to stable equilibria, dashed lines correspond to unstable equilibria and filled circles correspond to the largest and smallest values of* x *on a stable periodic orbit.* E_0 *represents the* $(0, 0)$ *equilibrium,* E_1 *is the* $(K, 0)$ *equilibrium and* E_* *is the* (x^*, y^*) *equilibrium.*

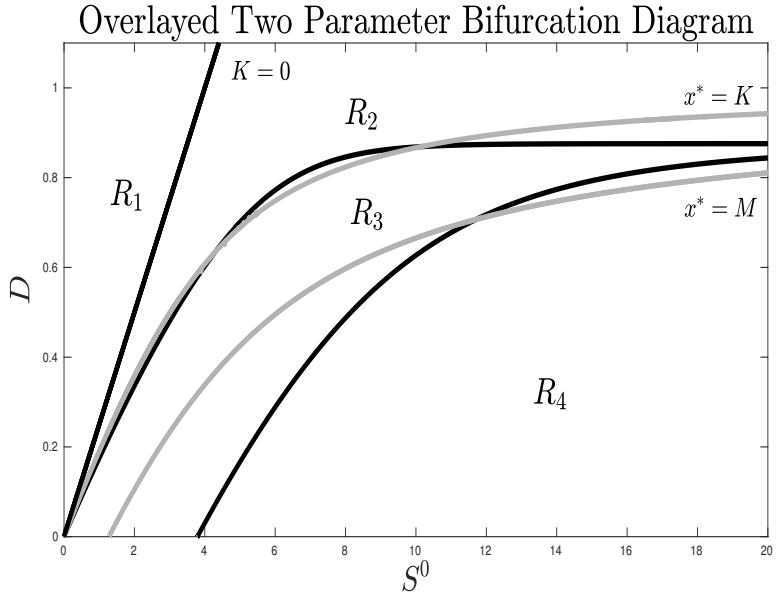

Figure 8.3: *Two parameter bifurcation diagrams for the Ivlev and Monod functional forms overlayed. The full opacity plot is Ivlev and the faded plot is Monod. The other parameters are set to* $m = 0.25$ *and* a *and* b *with the best fit values from Figure 8.1. In* R_1*, solutions converge asymptotically to* E_0*. In* R_2*, solutions with positive initial conditions converge to* E_1*. In* R_3 *solutions converge to the coexistence equilibrium* E_**. Finally, in* R_4 *solutions converge to a stable periodic orbit surrounding* E_**. The line separating* R_1 *and* R_2 *is the transcritical bifurcation between* E_0 *and* E_1 *that occurs when* $K = 0$*. The curve between* R_2 *and* R_3 *is the transcritical bifurcation when* E_1 *exchanges stability with* E_* *at* $x^* = K$*. The curve separating* R_3 *and* R_4 *is the Hopf bifurcation of* E_* *that occurs when* $x^* = M$*.*

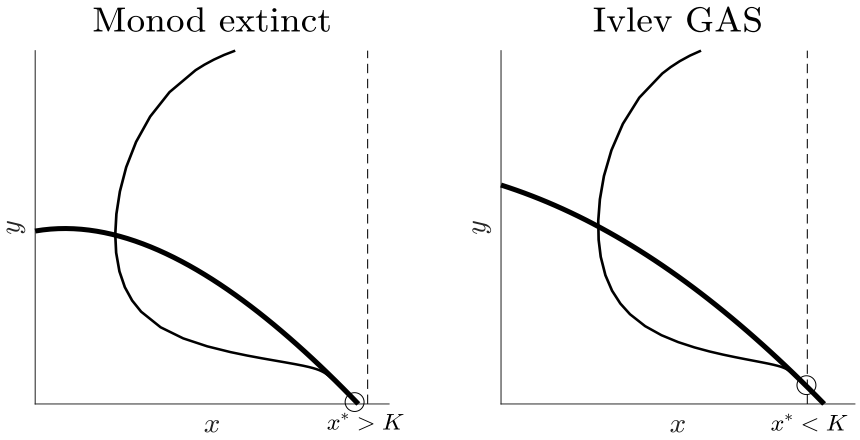

Figure 8.4: $S^0 = 5.1$, $m = 0.25$, $D = 0.7$, *a and b best fit parameters from Figure 8.1 gives rise to different dynamics. The initial condition in both figures is* $(1.5, 1)$. *For the Monod response we have extinction of the predator and convergence to the* $(0, K)$ *equilibrium. In the case of the Ivlev functional response, the coexistence equilibrium is a global attractor and both predator and prey populations persist.*

Fussmann and Blasius claim in [9] that when S^0 is increased in the classical Rosenzweig-MacArthur model, the different response functions have different degrees of destabilization. As they refer to it, destabilization of the system occurs when the dynamics change from a globally stable equilibrium point to a periodic orbit. They claim that the Monod functional response has a greater degree of destabilization than the Ivlev response, as S^0 is increased. By examining Figure 8.3, we can see that this is not the case. For smaller values of D we do observe that the system with Monod response will undergo its Hopf bifurcation before the Ivlev system does. However, as D is increased it is the Ivlev system which is first to reach the Hopf bifurcation. It is therefore incorrect to claim that either function has a higher degree of destabilization.

Without experimental data, it is impossible to determine whether the slight variations in where the bifurcations occur is actually statistically significant. It is entirely possible that the sensitivity observed here can be attributed to experimental error. Nevertheless, it is still surprising to note that even when the prey nullclines for both Monod and Ivlev responses are unimodal, differences in the dynamics of the system can still be found.

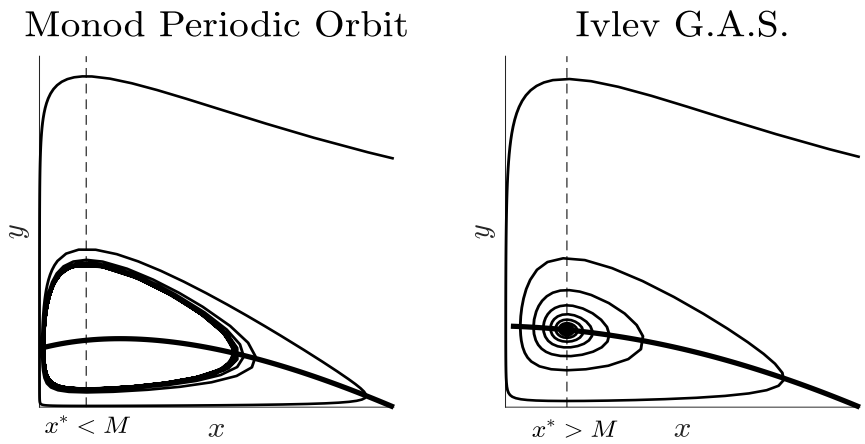

Figure 8.5: $S^0 = 4.5$, $m = 0.25$, $D = 0.3$, *a and b best fit parameters from Figure 8.1 gives rise to different dynamics. The initial condition for both panels is* $(9, 2)$. *Here, a periodic orbit is observed for the Monod response, but there is convergence to the coexistence equilibrium for the Ivlev response.*

Chapter 9

Discussion

In this thesis we have been concerned with establishing the dynamics of a chemostat predator-prey model with Ivlev functional response. We have also studied the sensitivity to the choice of functional response through a comparison between the dynamics with the Ivlev and Monod forms.

First we considered the possible configurations of the prey isocline. It was determined to be of Rosensweig-MacArthur form with at most one local extremum (a maximum). We also observed the existence of a unique inflection point when the isocline is initially concave up. It was determined that the local maximum moves up and to the right as the parameter K is varied.

The system was found to have three possible fixed points. The mutual extinction and the predator extinction equilibria are found to be saddle points when the coexistence equilibrium exists. The coexistence equilibrium is unstable when $x^* < M$ and locally asymptotically stable when $x^* \geq M$. A Lyapunov function extends local stability to global stability over a certain portion of the prey isocline. An application of the Dulac Criterion attempts to show that (x^*, y^*) is globally stable when it is locally stable, but relies on the assumption $\hat{\beta}'(x) > 0$ for $x > 0$.

By transforming our chemostat model into Liénard form we attempt to prove the uniqueness of the periodic orbit. This proof is missing a key piece of information as it relies on the function $f^*(u)$ only having three possible configurations. The shape of $f^*(u)$ remains to be rigorously proven, however in numerical experimentation no evidence to the contrary has been observed. This theorem could be useful in practical situations when parameter values are known.

In terms of bifurcations, this system was found to have two transcritical bifurcations and one Hopf bifurcation. The primary bifurcation parameter used was S^0. As S^0 was increased, stability transferred first from the $(0,0)$ equilibrium to the $(K,0)$ equilibrium via a transcritical bifurcation. The second transcritical bifurcation passed stability to the coexistence equilibrium, (x^*, y^*). Finally, continuing to increase S^0 caused the system to undergo a supercritical Hopf Bifurcation and a unique stable periodic orbit was observed. Both one and two parameter bifurcation diagrams were provided.

Through comparing the dynamics from the Ivlev and Monod responses the sensitivity of this model to specific functional forms was demonstrated. A complete proof for the uniqueness of the periodic orbit with the Monod functional response was provided. While the same sequence of bifurcations is observed in both cases, the bifurcations occurred for different parameter values. This would be an interesting area for further study. If numerical data could be obtained we would be able to understand if this sensitivity can be attributed to experimental error, or if it is, in fact, statistically significant.

In addition to analyzing experimental data to determine the authenticity of the differences in dynamics, some interesting further work would be to experiment with ratio dependent, rather than prey dependent, functional responses. Ratio dependent responses have the form $q(x/y)$, and it is compelling to find out if the sensitivity observed here persists. It would also be relevant to theoretically determine what is causing the sensitivity to functional form. Perhaps considering a one-parameter family of smooth functions from one functional response to the other could yield more insight in this area. Another idea could be to fix the values, slopes, and curvatures of the functional responses at the equilibrium values, and see how that affects the bifurcation values. It would also be interesting to search for practical applications with which the chemostat model is applicable, and examine if the sensitivity can actually be observed in nature.

Bibliography

[1] Aleksandr A. Andronov and A. Witt. Sur la théorie mathématique des auto-oscillations. *CR Acad. Sci. Paris*, 190:256–258, 1930.

[2] Geoffrey J. Butler, Herb I. Freedman, and Paul Waltman. Uniformly persistent systems. *Proceedings of the American Mathematical Society*, pages 425–430, 1986.

[3] Geoffrey J. Butler, Sze-Bi Hsu, and Paul Waltman. Coexistence of competing predators in a chemostat. *Journal of Mathematical Biology*, 17(2):133–151, 1983.

[4] Geoffrey J. Butler and Gail S. K. Wolkowicz. Predator-mediated competition in the chemostat. *Journal of Mathematical Biology*, 24(2):167–191, 1986.

[5] William A. Coppel. *Stability and asymptotic behavior of differential equations*. Boston, Heath, 1965.

[6] Paul K. Dayton, Gordon A. Robilliard, Robert T. Paine, and Linnea Dayton. Biological accommodation in the benthic community at McMurdo sound, Antarctica. *Ecological Monographs*, 44(1):105–128, 1974.

[7] Bard Ermentrout. *Simulating, Analyzing, and Animating Dynamical Systems: A Guide to XPPAUT for Researchers and Students*. SIAM, Philadelphia, 2002.

[8] Herb I. Freedman and Gail S. K. Wolkowicz. Predator-prey systems with group defence: The paradox of enrichment revisited. *Bulletin of Mathematical Biology*, 48(5-6):493–508, 1986.

[9] Gregor F. Fussmann and Bernd Blasius. Community response to enrichment is highly sensitive to model structure. *Biology Letters*, 1(1):9–12, 2005.

[10] Gary W. Harrison. Global stability of predator-prey interactions. *Journal of Mathematical Biology*, 8(2):159–171, 1979.

[11] Josef Hofbauer and Joseph W. H. So. Multiple limit cycles for predator-prey models. *Mathematical Biosciences*, 99(1):71–75, 1990.

[12] Eberhard Hopf. Abzweigung einer periodischen lösung von einer stationären lösung eines differentialsystems. *Ber. Math.-Phys. Kl Sächs. Akad. Wiss. Leipzig*, 94:1–22, 1942.

[13] Sze-Bi Hsu. On global stability of a predator-prey system. *Mathematical Biosciences*, 39(1):1–10, 1978.

[14] Xun-Cheng Huang. Uniqueness of limit cycles of generalised Liénard systems and predator-prey systems. *Journal of Physics A: Mathematical and General*, 21(13):L685–L691, 1988.

[15] Viktor S. Ivlev. *Experimental ecology of the feeding of fishes*. Yale University Press, 1964.

[16] Alan D. Jassby and Trevor Platt. Mathematical formulation of the relationship between photosynthesis and light for phytoplankton. *Limnology and Oceanography*, 21(4):540–547, 1976.

[17] Robert E. Kooij and André Zegeling. A predator–prey model with Ivlev's functional response. *Journal of Mathematical Analysis and Applications*, 198(2):473–489, 1996.

[18] Robert E. Kooij and André Zegeling. Qualitative properties of two-dimensional predator-prey systems. *Nonlinear Analysis: Theory, Methods and Applications*, 29(6):693–715, 1997.

[19] Joseph P. LaSalle. Some extensions of Liapunov's second method. *IRE Transactions on circuit theory*, 7(4):520–527, 1960.

[20] Alfred-Marie Liénard. Etude des oscillations entretenues. *Revue gnrale de l'lectricit 23, pp. 901912 and 946954*, 1928.

[21] Alfred J. Lotka. Contribution to the theory of periodic reactions. *The Journal of Physical Chemistry*, 14(3):271–274, 1910.

[22] Maple. *Maplesoft, a division of Waterloo Maple Inc.* Waterloo, Ontario, 2015.

[23] Jerrold E. Marsden and Marjorie McCracken. *The Hopf bifurcation and its applications*, volume 19. Springer Science and Business Media, 2012.

[24] MATLAB. *version 9.1 (R2016b)*. The MathWorks, Inc., Natick, Massachusetts, 2016.

[25] Jacques J. Monod. The growth of bacterial cultures. *Annual Reviews in Microbiology*, 3(1):371–394, 1949.

[26] Michael L. Rosenzweig. Paradox of enrichment: destabilization of exploitation ecosystems in ecological time. *Science*, 171(3969):385–387, 1971.

[27] Michael L. Rosenzweig and Robert H. MacArthur. Graphical representation and stability conditions of predator-prey interactions. *The American Naturalist*, 97(895):209–223, 1963.

[28] Gunog Seo and Gail S. K. Wolkowicz. Sensitivity of the dynamics of the general Rosensweig MacArthur model to the mathematical form of the functional response: A bifurcation approach. *Pre-print*, 2016.

[29] Hal L. Smith and Paul Waltman. *The theory of the chemostat: dynamics of microbial competition*, volume 13. Cambridge University Press, 1995.

[30] Peter Turchin. *Complex population dynamics: a theoretical/empirical synthesis*, volume 35. Princeton University Press, 2003.

[31] Vito Volterra. *Variazioni e fluttuazioni del numero d'individui in specie animali conviventi*. C. Ferrari, 1927.

[32] Zhang Zhifen. Proof of the uniqueness theorem of limit cycles of generalized Liénard equations*. *Applicable Analysis*, 23(1-2):63–76, 1986.